

## Structure in the 3D Galaxy Distribution: II. Voids and Watersheds of Local Maxima and Minima

M.J. Way<sup>1,2</sup>, P.R. Gazis and Jeffrey D. Scargle

*NASA Ames Research Center, Space Science Division, Moffett Field, CA 94035, USA*

Michael.J.Way@nasa.gov, PGazis@sbcglobal.net, Jeffrey.D.Scargle@nasa.gov

### ABSTRACT

The major uncertainties in studies of the multi-scale structure of the Universe arise not from observational errors but from the variety of legitimate definitions and detection methods for individual structures. To facilitate the study of these methodological dependencies we have carried out 12 different analyses defining structures in various ways. This has been done in a purely geometrical way by utilizing the HOP algorithm as a unique parameter-free method of assigning groups of galaxies to local density maxima or minima. From three density estimation techniques (smoothing kernels, Bayesian Blocks and self organizing maps) applied to three data sets (the Sloan Digital Sky Survey Data Release 7, the Millennium Simulation and randomly distributed points) we tabulate information that can be used to construct catalogs of structures connected to local density maxima and minima. The resulting sizes follow continuous multi-scale distributions with no indication of the presence of a discrete hierarchy. We also introduce a novel void finder that utilizes a method to assemble Delaunay tetrahedra into connected structures and characterizes regions very nearly empty of galaxies in the source catalog.

*Subject headings:* multi-scale structure, galaxy clusters, voids

### Contents

<b>1</b>	<b>Introduction</b>	<b>2</b>
<b>2</b>	<b>Previous Work</b>	<b>4</b>

---

<sup>1</sup>NASA Goddard Institute for Space Studies, 2880 Broadway, New York, NY, 10025, USA

<sup>2</sup>Department of Astronomy and Space Physics, Uppsala, Sweden

<b>3</b>	<b>Identification of Structures</b>	<b>6</b>
3.1	The HOP Algorithm . . . . .	8
3.2	Delaunay Tetrahedra as Void Tracers . . . . .	12
3.3	Ambiguity, Uncertainty, Noise and Persistence . . . . .	15
3.4	Structures Obtained with the HOP Algorithm . . . . .	17
3.5	Some Properties of Delaunay Voids . . . . .	24
<b>4</b>	<b>Conclusions</b>	<b>28</b>
<b>5</b>	<b>Appendix A: Data Details</b>	<b>31</b>
5.1	The SDSS NASA/AMES Value Added Galaxy Catalog (AMES-VAGC) . . . . .	31
5.2	Stage 1: Extracting tables from the SDSS NYU-VAGC . . . . .	31
5.3	Stage 2: Obtaining a contiguous and volume limited sample . . . . .	32
5.4	Stage 3: 55" fiber placement issue and coordinate transform . . . . .	33
5.5	Stage 4: Voronoi related calculations . . . . .	33
5.6	Stage 5: Flagging boundary points . . . . .	34
5.7	Stage 6: Building a table for casjobs . . . . .	34
5.8	The adaptive kernel map classes . . . . .	35
5.9	The Millennium Simulation AMES Value Added Catalog . . . . .	35
5.10	The Randomly Distributed Point Catalog . . . . .	36
5.11	Structure Catalog Information: Electronic-Only Files . . . . .	39
5.12	Void Catalog Information: Electronic-Only Files . . . . .	44
<b>6</b>	<b>Appendix B: Zwicky Morphological Analysis of Topological Noise Effects</b>	<b>44</b>

## 1. Introduction

In the last two decades an assortment of disparate density estimation techniques has been applied to a wide variety of data sets to characterize the distribution of galaxies in the local universe. From the very beginning the purely geometrical studies were supplemented by studies of cluster luminosity functions (e.g. Holmberg 1969, and references therein to earlier work by

Zwicky). While these studies have been productive, systematic inter-comparison of the results continues to be problematic. The purpose here is to address this problem by presenting data for the construction of catalogs drawn from three data sources: the Sloan Digital Sky Survey (York et al. 2000, hereafter SDSS), the Millennium Simulation (Springel et al. 2005, hereafter MS) and a set of randomly distributed points. Each of these data sets were analyzed in three different ways. These are the same data and analysis techniques described in the first paper in this series (Way et al. 2011, hereafter Paper I).

The first of these data sets allows elucidation of the structure of the actual galaxy distribution. Technology implementing fully digital, charge-coupled device (CCD) photometric and spectroscopic observations of large areas of the sky has yielded a cornucopia of surveys of the local universe in the past 15 years: e.g. LCRS<sup>3</sup>, 2MASS<sup>4</sup>, 2dFGRS<sup>5</sup>, and SDSS. A variety of density estimation techniques have been proposed and used to elicit structural information from these data compendia. Many of the methods and the catalogs they have yielded were recently discussed in Paper I. However, observational surveys continue to grow larger and more elaborate, with cumulative releases coming every 6 months to 1 year. For example the SDSS is at Data Release 10 as of August 2013 (Ahn et al. 2013, DR10). The DR10 is part of the SDSS 3<sup>6</sup> survey scheduled to collect data through 2014. The complexities and sheer numbers of both surveys and analysis methods make evaluation and interpretation of results, and the corresponding inter-comparisons, ever more difficult. Even the restricted arena of density representations is replete with different estimation techniques (of which we discuss three) and approaches to subsequent characterization of the density field (*cf.* §3).

To address this circumstance we have performed spatial structure analysis of three directly comparable point data sets (measured, simulated, and random galaxy positions) using three density estimation techniques (adaptive kernels, self-organized maps, and Bayesian blocks). We hope these analyses will be of use to researchers in making comparisons among their own methods and those described here, on a variety of redshift surveys. All elements of the corresponding nine-fold matrix (3 data sets  $\times$  3 analysis methods) were described in Paper I. Detailed characteristics of the data are described in Appendix A (Section 5).

This paper describes our procedure for converting density estimates into localized features in the spatial distribution of galaxies. As described in Paper I this result is achieved by assembling building blocks (tessellation cells or blocks of them) into larger structures. A key point is that both the localized details and global features that result are dependent on the principles under which this assembly is carried out. Hence one of the key goals is to understand the nature of

---

<sup>3</sup>Las Campanas Redshift Survey (Shectman et al. 1996), although they did not actually use CCDs for their spectroscopy.

<sup>4</sup>Two Micron All Sky Survey (Skrutskie et al. 2006)

<sup>5</sup>The Two Degree Field Redshift Survey (Colless et al. 2001)

<sup>6</sup><http://www.sdss3.org>

this dependence in order to elucidate the astrophysical meaning of conclusions about the origin, evolution and current nature of the cosmic web. In the literature these structures are typically assigned to four classes: clusters, sheets, filaments and voids. Our analysis leads to the point of view that the *cosmic web* (e.g. van de Weygaert et al. 2009) is composed of a random array of structures of widely distributed shapes not necessarily assignable to these four classes in a straightforward way.

## 2. Previous Work

A number of recent publications have described methods for identifying and characterizing structure in redshift surveys and simulations. For some developments since the summary in Paper I see e.g. Aragon-Calvo et al. (2010a); Cautun (2011); Sousbie et al. (2011); Sousbie (2011, 2013); Falck, Neyrinck & Szalay (2012); Knebe et al. (2013); Tempel et al. (2014) and with respect to tessellation methods Schaap (2007); Pandey et al. (2013); Angulo et al. (2013). For a comparative study of density estimation schemes see Platen et al. (2011), and for an example of machine learning approaches see D’Abrusco et al. (2012).

Because voids were not discussed in Paper I, a brief review of the literature on this topic is in order. The concept of under-densities in the distribution of galaxies and the related term *void* has been around at least since the late 1970s. Not unexpectedly this early work was characterized by vague definitions and uncertainties due to small sample sizes. Some of this confusion continues to today.

Chincarini & Rood (1976) conducted one of the first observational studies indicating the presence of voids in distribution of galaxies (for  $m \lesssim 15$ ) in the region of the Coma Supercluster. They described the effect as a “segregation in redshifts,” but it is now known that their survey was deep enough to see actual voids.

The first explicit mention of voids or holes in the galaxy distribution can probably be shared between that of Gregory & Thompson (1978) and that of Joeveer et al. (1977, 1978). The former was published in 1978, while the latter were a pre-print from 1977 and its accepted version in 1978. The Joeveer et al. (1977) pre-print was also distributed in the Fall of 1977 amongst participants at IAU Symposium No. 79 in Talinn, Estonia. For more detail on this time period see Einasto (2014, p.138) and Thompson & Gregory (2011).

By the time of the 1977 IAU Symposium in Talinn, Estonia (Longair & Einasto 1978) voids or holes were common parlance amongst the community. Here we present a number of examples of the relevant references. Tully & Fisher (1978) Table II document a *void* of  $>1000$  Mpc<sup>3</sup>. Joeveer & Einasto (1978) use the words *void* and *holes* in their 1978 IAU paper, and estimate on page 247 that “Cell interiors are almost void of galaxies; they form big holes in the Universe with diameters of 100–150 Mpc.” Tift & Gregory (1978) say on page 267 that “There are regions more than 20Mpc in radius which are totally devoid of galaxies.” and “The foreground is again

very clumpy with one major void of radius close to 40Mpc.” Zeldovich (1978) recognizes the large empty spaces (holes) discussed by others at the conference while Longair (1978) in his conference summary also mentions on page 455 “... holes which are about 10 Mpc in size and void of bright galaxies.” See also Schwarzschild (1982) and a more recent overview of the void phenomenon by Peebles (2001).

In a pioneering mathematical study<sup>7</sup> of probabilities that a randomly placed region of given volume will contain a given number (including zero) of galaxies White (1979) noted that the distributions of dense structures and voids are related to each other.

According to Martinez & Saar (2002, p.368) the first (systematic) study of voids by Einasto et al. (1989) was an attempt to establish the fractal character of the galaxy distribution. These authors developed the *empty sphere method*, thus pioneering methods to search directly for empty or near-empty volumes.

This approach threads the series of papers by El-Ad et al. (1996); El-Ad (1997); El-Ad & Piran (1997) discussing the observational discovery of voids with the *Void Finder* algorithm (see also Hoyle & Vogeley (2002) for an extension of this approach). For automatic detection of voids in redshift surveys such as the IRAS catalog see El-Ad et al. (1997). The study of El-Ad & Piran (2000) is of particular interest because of its comparison of voids discovered in two independent surveys at different wavelengths. All of this work apparently influenced later methodological work close in spirit to that developed here, involving variations on explicit search for volumes actually devoid of galaxies (Kauffmann & Fairall 1991; Aikio & Mahonen 1998; Elyiv et al. 2013; Tavasoli et al. 2013), via nearest neighbor techniques (e.g. Rojas et al. 2004) or “friends-of-friends” algorithms (e.g. Muñoz-Cuartas & Müller 2012).

In much other work the definition of voids is tied to local minima in the density distribution, e.g. the Watershed Void Finder (WVF) (see Platen et al. 2007, and references therein), VOBOZ (VOronoi BOund Zones) (Neyrinck et al. 2005), and ZOBOV (Zones Bordering on Voidness) (Neyrinck 2008). These works and their concept of *watersheds* are closely related to the core idea of the HOP (Eisenstein & Hut 1998) algorithm adopted here. The two classes of void finders – based on empty volumes or local density minima – have their advantages and disadvantages. The former is naturally aligned with the discrete tessellations without smoothing that characterizes our previous work in Paper I. See also the recent works by Neyrinck et al. (2013) and Nadathur & Hotchkiss (2014).

Schmidt et al. (2001) deal with voids in simulations, comparing methods based on finding empty regions of space (within observational limits and selection effects in the survey) against those based on density estimation followed by identification of density minima. They also include two different void finder algorithms with and without predefined constraints on shape. Extensive

---

<sup>7</sup>This work was apparently inspired by White’s perception of ‘holes’ in the galaxy distribution depicted in Gregory & Thompson (1978).

studies of the structure and dynamics of voids (Aragon-Calvo et al. 2010b; Aragon-Calvo & Szalay 2013) argue for the existence of a hierarchical distribution of voids in the context of the *cosmic web* and *cosmic spine* concepts (see also Aragon-Calvo et al. 2007, 2010a). While the term *hierarchy* is commonly invoked for both voids and structures no evidence for discrete levels is found in analysis of survey data. We feel that the distributions of sizes of structures are better described as continuous and multi-scale, not hierarchical (cf. the comments in Section 4.)

A number of recent works have investigated the statistics and stacking of voids and their importance for various environmental and other cosmological issues (Hahn et al. 2007a,b; D’Aloisio & Furlanetto 2007; Gaite 2009; Paranjape et al. 2009; Lavaux & Wandelt 2010; Einasto et al. 2011; Pan et al. 2012; Einasto et al. 2012; Bos et al. 2012; Lavaux & Wandelt 2012; Bolejko et al. 2012; Zaninetti 2012; Varela et al. 2012; Sutter et al. 2012; Jennings et al. 2013; Beygu et al. 2013; Krause et al. 2013; Ceccarelli et al. 2013; Hamaus et al. 2013; Ricciardelli, Quilis and Varela 2014; Hamaus et al. 2014). A comparison of void catalogs and detection methods applied to the MS data is found in Colberg et al. (2008); see also Knebe et al. (2011). And more generally, powerful methods of point process theory (Daley & Vere-Jones 2003; Lowen & Teich 2005), stochastic geometry (Snyder & Miller 1991), discrete Morse theory (Sousbie 2011, 2013), computational (de Berg et al 1997; Preparata & Shamos 1985) and combinatorial geometry (Edelsbrunner 1987), and wavelet-like transforms (Leistedt et al. 2013) are currently being used to explicate multi-scale structures in the galaxy distribution (van de Weygaert et al. 2011a,b,c; Sousbie et al. 2011; Sousbie 2011, 2013; Park et al. 2013; Hidding, Shandarin & van de Weygaert 2014). Especially interesting are the prospects for studying voids via gravitational lensing effects (Amendola et al. 1999; Higuchi et al. 2011; Melchior et al. 2013).

### 3. Identification of Structures

The grand challenge is to produce scientifically useful characterization of a density field derived from a galaxy survey or a computational dark matter simulation. One approach is to study statistical quantities averaged over the hole data sample. Examples include estimation of correlation functions (McBride et al. 2011; Valageas & Clerc 2012; Müeller et al. 2012), power spectra (Tegmark et al. 2006; Jasche et al. 2010; Neyrinck et al. 2009), and global topological information (Shandarin et al. 2004; Gott et al. 2008; James et al. 2009; van de Weygaert et al. 2010; Sousbie 2011; Sousbie et al. 2011; Einasto et al. 2014). Here instead we develop an alternative approach, namely identification of specific local features of the density distribution, as outlined in Figure 1.

In Paper I the steps on the left side of the figure yielded density surrogates for individual galaxies or small sets of them. The current paper addresses the assembly of these building blocks into structures.

It is under-appreciated that the results of any such analysis are very dependent on the methodology used. Especially strong is the dependence on the assembly procedure, but all of the choices represented in Figure 1 have their effects. There is a plethora of definitions of structural classes

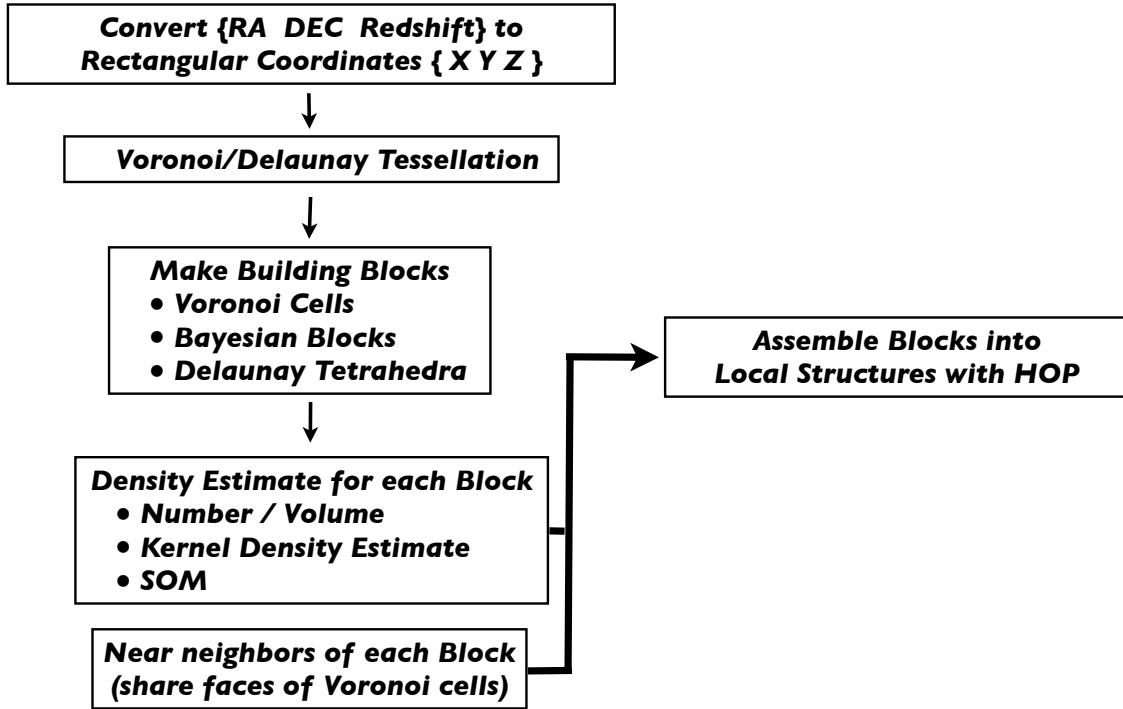


Fig. 1.— Flow chart for the analysis procedure. Processes on the left were described in Paper I; assembling building blocks into structures is the main topic of the current paper. The tessellation techniques and self-organizing maps (SOM) are as in Paper I. HOP (Eisenstein & Hut 1998) is the assembly algorithm adopted here.

and approaches to detecting them, using a variety of positional, photometric and morphological information. In particular some detection algorithms, such as those invoking prior information about galaxy colors or cluster symmetry, naturally favor detection of structures more nearly satisfying these assumed properties. This rather murky situation raises questions. Are there intrinsic distinct well-defined structural classes? If there are, can we uncover their nature in objective ways not unduly influenced by methodology and prior assumptions? Since structures can have, macroscopically speaking, four possible dimensions (0, 1, 2, and 3) the corresponding shape classes – clusters, filaments, sheets, and voids – seem natural. This classification scheme has been adopted by the community, with some recognition that shapes are somewhat randomly distributed in and between these categories. In any case it is important to exercise care in the interpretation of structural results. Comparison of observed and simulated data using identical analyses is inherently less ambiguous, but even such comparative studies depend on the nature of the analysis.

Our work seeks to avoid some of this murkiness by using purely geometrical information derived from galaxy positions, and in ways not tuned to emphasize any particular shape. The approach here is to characterize structure over a range of scales, i.e. *multi-scale structure* (a more precise term than the commonly used *large-scale structure*). We aim to make maximal use of the information in the data, but with neither prior shape constraints nor account of geometrically extraneous systematics such as the *red sequence* in clusters (Gladders & Yee 2000; Rykoff et al. 2013; Rozo & Rykoff 2013; Rykoff et al. 2014). We adopt what is arguably the simplest possible definition: *a structure is the watershed of a single critical point* – that is of a local density maximum or minimum (see Section 3.1 for specifics). This choice rules out structures with two peaks e.g., but if desired these could be sought during a post-processing with some kind of merger criterion. Identification of voids via local density minima is supplemented with a novel void finding procedure in Section 3.2. In a further bid toward objectivity and parameter freedom we use tessellation techniques so that the scale on which these maxima are determined is automatic, data-adaptive, and not predefined. The full definition of structures then requires a prescription for what to attach to the local maxima or minima. Here we assemble structures out of elementary building blocks as outlined in Section 4.3.3 of Paper I, avoiding arbitrary choices through the use of the parameter-free HOP algorithm of Eisenstein & Hut (1998).

### 3.1. The HOP Algorithm

The rest of this paper is devoted to the process of assembling structures out of building blocks (cf. the right-hand side of Figure 1). The next subsection describes a general algorithm for assembling local structures in any data representation consisting of these three elements:

- (1) A set of discrete entities, called *objects*
- (2) The value of a function  $\mathbf{f}$  for each object
- (3) Adjacency information among the objects

We refer to  $\mathbf{f}$  as the *HOP function*. For the computations only the last two items matter, as the algorithm makes no reference to the identity of the objects. In continuous Morse theory (Milnor 1969) the *Morse function* – the analog of our  $\mathbf{f}$  – must be infinitely differentiable; in the discrete theory of Forman (2002) the corresponding function must satisfy some similarly delicate conditions. Here in contrast the HOP function is essentially arbitrary since it only needs to provide an ordering of the objects. Hence the only condition on  $\mathbf{f}$  is that no two objects are assigned the same value; violations of this constraint can be fixed in a trivial way.

In some of the cases reported here the objects are individual galaxies, with the HOP function given by a density value assigned to each one (e.g via Voronoi cell volumes, kernel density estimates, or SOM class identifiers related to density). In another – the case of Bayesian Blocks (Scargle et al.



2013) – the objects are connected sets of adjacent galaxies with the appropriate density estimate (number of galaxies in the block divided by its volume). In the final example considered here, where the objects are the Delaunay tetrahedra in the tessellation of galaxy positions, the definition of  $\mathbf{f}$  requires some thought, as elaborated in Section 3.2.

For the adjacencies referred to in item (3) above we use those defined by the Voronoi tessellation itself, as follows: two objects, either individual Voronoi cells or blocks thereof, are deemed adjacent if they intersect at a common face.<sup>8</sup> This construct can be viewed as defining nearest neighbors in a data-adaptive fashion, with no a priori restriction on the number of neighbors. It thus conveys local information regarding the distribution of galaxies more efficiently than say nearest-neighbors with a pre-defined number of neighbors. Similarly two Delaunay tetrahedra are considered adjacent if they share a common triangular face.

Identification of watershed structures in a spatial distribution of objects is conveniently implemented using the group-finding algorithm HOP (Eisenstein & Hut 1998). Here by the term HOP we mean only the group-finding step (their Section 2.1) distinguished from data smoothing and merging of groups discussed elsewhere in their paper. Aubert, Pichon & Colombi (2004) describe a variant of this post-processing, called **AdaptaHOP**; their approach differs in many ways from ours, such as regarding the sampling as noise to be smoothed over, and has procedures that generate hierarchical leaves in a tree. See also Springel (1999) for a discussion of a related algorithm called **SUBFIND**. Motivated by the requirements for analysis of massive cosmological data sets, Skory et al. (2010) deals with computational parallelization issues. Turk et al. (2011) provide a toolkit that contains an implementation of HOP.

This algorithm is quite general. For any given HOP function and adjacencies defined for each object in set  $\mathbf{S}$ , it yields a partition of  $\mathbf{S}$  into groups with these properties:

- (a) The elements of the partition, here called *groups*, are sets of objects from  $\mathbf{S}$ .
- (b) There is one such connected group for each local maximum of  $\mathbf{f}$ .
- (c) In a given group  $\mathbf{f}$  decreases monotonically away from the maximum.
- (d) Every object is in one and only one of the groups (i.e., the groups partition the space).
- (e) The partition is unique and parameter-free.

In short HOP identifies all of the local maxima of  $\mathbf{f}$  and the connected structures flowing from them; together these are the discrete analog of the so-called *descending manifolds* – mountain peaks

---

<sup>8</sup>Objects being joined by an edge in the Delaunay tessellation is equivalent to this condition (but not to other possible definitions such as sharing Voronoi edges or vertices in lieu of faces). These adjacencies are easily established from information supplied by most data analysis systems, such as the n-dimensional MatLab routine *voronoin*, namely identities of the vertices of each Voronoi cell. In finding adjacencies it is very useful to first compile a list of all galaxies whose Voronoi cells touch each vertex.

plus their watersheds. It can identify structures of any shape – containing arbitrary mixtures of convexities and concavities, possibly even failing to be simply connected. The underlying idea of HOP is a simple hill climbing prescription. It iteratively associates each object with neighbors that have larger values of  $\mathbf{f}$  according to this formulation:

### The HOP Algorithm (Eisenstein & Hut 1998)

Given: A set  $\mathbf{S}$  of  $N$  spatially distributed data objects  $\mathbf{o}_i, i = 1, 2, \dots N$

- (1) Establish an index array  $\mathbf{I} = \{1, 2, 3, \dots N\}$  for any convenient ordering of the objects.
- (2) Assign a value of  $\mathbf{f}$  to each object.
- (3) For each object identify all objects adjacent to it, i.e. its spatial neighbors as defined earlier in this section.
- (4) For each set consisting of an object and all of its neighbors, find the object with the largest value of  $\mathbf{f}$ .
- (5) Iterate as follows:
  - (a) For  $i = 1, 2, \dots N$ :
    - (i) Let  $\mathbf{j}_i$  be the current index value in position  $i$  of  $\mathbf{I}$
    - (ii) In  $\mathbf{I}$  replace  $\mathbf{j}_i$  with with that found in (4) for object  $\mathbf{j}_i$  (not that for object  $i$ )
  - (b) Repeat (a) until no index value changes
- (6) Set  $\mathbf{K} = \mathbf{I}$  with duplicate values removed.

Eliminating the duplicate values in the converged  $\mathbf{I}$  yields a set of indices  $\mathbf{K}$  pointing one-to-one to each of the local density maxima – objects denser than all of their neighbors. Each of the objects ends up pointing via the converged  $\mathbf{I}$  to one and only one of these maxima (i.e. to one of the values in  $\mathbf{K}$ ). This property generates for each local maximum a connected structure, consisting of a set of paths connecting adjacent galaxies along which the density is monotonic. These structures are much like the *watersheds* defined in image processing and many of the cosmic web algorithms referenced above.

In short this algorithm uses a simple hill climbing procedure to find a unique partition of the objects into groups, one associated with each of the local maxima. Alternatively, by jumping instead to the neighbor with the smallest value of  $\mathbf{f}$  in Step 4 HOP can find basins of attraction for all of the local *minima* instead. We usually refer to structures associated with local maxima as *groups*, rather than clusters, since they may e.g. be filamentary or sheet-like. With a similar freedom with standard terminology, drainage basins associated with local minima can be called

*voids*, although we distinguish these structures from the empty collections of Delaunay tetrahedra discussed in Section 3.2.

The following MatLab code fragment uses vector operations to implement the iteration, given two arrays initialized as follows:

```
index = [1, 2, ... N] contains the initial indices of the objects (taken in arbitrary order)
id_max_neighbor contains indices of the neighbors found in step 4

while 1
    index_new = id_max_neighbor( index );    % Each object hops to highest neighbor
    id_change = find( index_new ~= index ); % Locate index changes
    if isempty( id_change );break;end       % If no index changes escape while loop
    index = index_new;                      % Implement changes due to hops
end
```

We take the objects in  $\mathbf{S}$  to be individual galaxies, blocks containing several galaxies, or Delaunay tetrahedra – attached to which are values of  $\mathbf{f}$ . This function is given by the corresponding KDE or BB density estimates, classes from the SOM method, or derived from the sizes of the Voronoi cells or Delaunay tetrahedra.

The following points elaborate some details of the algorithm and our application of it.

1. Choices for the definition of the neighbor relation in step 3, and indexed by `id_max_neighbor`, include densest neighbor (to find manifolds descending from local maxima) and least dense neighbor (to find manifolds ascending from local minima).
2. Throughout this discussion there is no explicit mention of the dimensionality of the data. One of the beauties of the HOP algorithm is that it applies to spaces of any dimension. Here contact with the dimension of the data arises only in the definition of adjacency, which we compute from the Voronoi tessellation of the 3D galaxy positions. But once the adjacencies are assigned dimension is completely irrelevant.
3. The unique output of this algorithm is independent of the order of the initial indexing (1) or the order in which the objects are considered in step (5), modulo an inconsequential re-ordering of the output groups.
4. The iteration can be carried out in other ways than shown explicitly above, e.g. by following individual objects to their final destinations, rather than the parallel procedure in (5)(a). Such path tracking is of use for constructing analogs of topological saddle points, not discussed here.
5. If two or more objects are assigned identical values, rare except in the case of the discrete SOM class identifiers, there may be a dependence on the way the resulting ambiguity is resolved.

6. After the preprocessing represented by the initial steps (1) - (4), iteration (5) is guaranteed to converge rapidly because of the monotonic nature of the bounded upward jumps, which are the source of the name HOP.
7. All that matters is the ordering of the function values, so  $\mathbf{f}$  can be replaced with ordinal numbers. i.e. integers indexing the array  $\mathbf{f}$  in increasing order.
8. The first step of the ZOBOV algorithm (Neyrinck 2008) and most Morse theory algorithms is based on what is essentially the same as HOP.
9. There is no loss of information due to smoothing in the process of assembly of objects into structures, although Bayesian Blocks can be thought of as a form of smoothing (more properly “chunking”) in preprocessing.
10. HOP is a major simplification, sidestepping much of the complexity of Morse theory (continuous or discrete) and persistency concepts that characterize modern topological data analysis (cf. references in Section 2).
  - Nonetheless the results presented here compare favorably to those from more elaborate algorithms, for example based on discrete Morse theory. The essential difference is that small structures, discarded by others because they are not *persistent* as some parameter is varied, we regard as conveying important information and are therefore retained in our analysis
  - One concern is that our resulting structures might extend from their defining local maxima down to low density levels that might be better assigned to local minima. Some aspects of topological data analysis address this issue by truncating structures, utilizing saddle points and intersections of ascending and descending manifolds. However, the structures found here without such procedures do not seem to have any pathological features, such as tentacles extending far from the defining critical point.

Before showing examples of structures determined with HOP, the next section describes some considerations relevant to another way to detect voids.

### 3.2. Delaunay Tetrahedra as Void Tracers

As described in Section 1 the so-called *voids* in the galaxy distribution have been the subject of considerable study. These features are informative regarding the multi-scale structure of the Universe, just as are dense structures. A variety of definitions of voids, and detection methods keyed to the defining characteristics, provide different views of both individual and overall structures. As discussed above in Section 2 some detection methods focus on local density minima; others locate volumes of space empty of galaxies within the limits of the survey or simulation, with no explicit

reference to local minima in a continuous density representation. We here develop an approach of this latter kind that we believe is novel in its explicit use of Delaunay cells as the building blocks for the voids.

Delaunay and Voronoi tessellations are *duals*<sup>9</sup> to one another, each partitioning the data space into small sub-volumes in different ways but elucidating similar spatial information. We have seen that cells in a Voronoi tessellation of galaxy positions are good building blocks for constructing a representation of the corresponding density field. However Delaunay tessellation is much more effective than Voronoi tessellation for void detection. The toy example in Figure 2 compares their responses to an artificial empty region in a set of otherwise random 2D points. The strategy is to find an objective way to identify a set of cells approximating the void, for example by selecting those cells larger than some adopted size threshold.

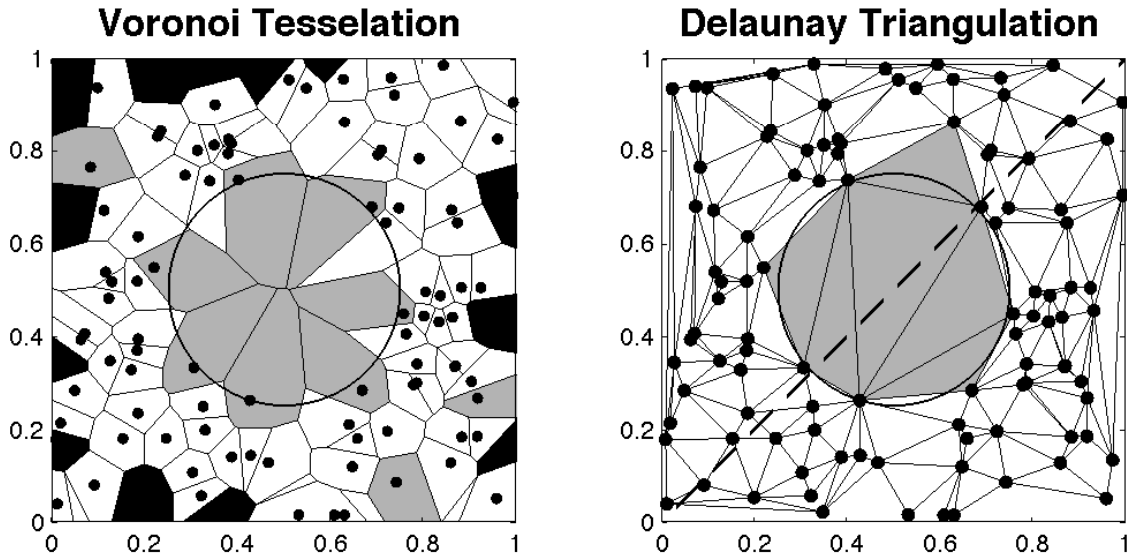


Fig. 2.— Tessellations for a synthetic 2D circular void. Points shown as dots are randomly and uniformly distributed in the unit square excluding a circle of radius  $\frac{1}{4}$ . Left: Voronoi cells with areas  $> .023$  and  $> .05$  are shaded gray and black. Right: Delaunay triangles with areas  $> .019$  shaded gray. (The thresholds were chosen to roughly optimize the void representations.)

Several problems beset Voronoi tessellation’s partial success in the left panel. Identification

---

<sup>9</sup>This concept refers to several relations. See (Okabe et al. 2000) for details.

of void cells is relatively complicated. Both upper and lower thresholds are required, the putative void cells shown in gray lying in between. The cells above the upper threshold (black) are oversized due to edge effects (cf. Paper I) and those below the lower threshold (white) are in the denser non-void region. Typically there is no range of cell areas that includes all the cells in the void and only those cells – that is rejecting both edge and extra-void cells. In the left panel of Figure 2 three obvious edge cells are incorrectly denoted as void cells (grey). Adjusting the upper area threshold to correct this mistake eliminates some true void cells. Even the best Voronoi coverage does not provide a very exact representation of the void’s shape and extent. Finally, since they must contain a data point, the identified void cells not only extend outside the true circular void but they carry a nontrivial density, namely unity divided by the cell area. On the other hand in the Delaunay triangulation (Figure 2, right panel) the circular void is well represented using a single area threshold yielding a small number of triangles, each of which is empty and can be interpreted as carrying zero density.

Furthermore sets of several contiguous Delaunay tetrahedra typically make up structures devoid of galaxies. Figures 2 and 3 show quirky 2D examples of this fact. In the right panel of Figure 2 the dashed line running diagonally between the lower-left and upper-right corners does not obviously define a structure of any interest, but in fact the set of Delaunay triangles which it intersects is a void in the form of jagged polyhedron not containing any of the points. Figure 3 demonstrates the same thing for triangles intersected by a continuous curve (not shown) in the plane. Neither of these shapes are what one thinks of as reasonable voids, but as discussed in Section 3.3 this does not mean that they are somehow not real. In principle collections of adjacent tetrahedra are not necessarily empty of galaxies (cf. Section 3.5) but in the analyses presented here they always are.

The 2D toy examples in Figures 2 and 3 were chosen for ease of visualization but these conclusions are even more definitive in 3D: many paths similarly define snake-like connected configurations of empty Delaunay tetrahedra (cf. Figure 3). Detected void structures are very sensitive to the assembly process, as was evident in the Aspen-Amsterdam void finder comparison project. The void volume fractions with the various void finders reported in column 4 of Table 2 of Colberg et al. (2008) range from 0.13 to 1.0. The last number, due to Platen and Van de Weygaert, means the entire data space is represented as a single highly convoluted but empty polyhedron. With a goal of identifying coherent low density structures an obvious scheme is to start from locally largest Delaunay tetrahedra and apply criteria for attaching one or more of the 4 face-sharing neighbors, perhaps based on something like size, shape or distance. To avoid subjectivity of such ad hoc procedures we use HOP’s prescription for partitioning the set of tetrahedra comprising the Delaunay tessellation (Section 3.4). To do this we need a new definition of the function  $\mathbf{f}$  in algorithm 3.1, since a surrogate for galaxy density is not appropriate for void finding. In order to represent the degree of emptiness we take  $\mathbf{f}$  equal to tetrahedron volume. In much the same way that small Voronoi cells correspond to large density, large Delaunay cells correspond to a large degree of emptiness.<sup>10</sup>

---

<sup>10</sup>Tessellation ameliorates dependencies on the size of the region sampled. “... if you want to measure the density

### 3.3. Ambiguity, Uncertainty, Noise and Persistence

Quantifying uncertainty in data analysis requires careful assessment of any process affecting the signal of interest, either randomly or systematically, anywhere along the entire chain leading from raw measurements to the final estimate. In addition subsequent interpretation must allow for dependencies of the results on the analysis method. Accordingly at least the following issues need to be considered in assessing the cosmological significance of the present analysis:

- (1) Errors in measured sky positions and redshifts of individual galaxies.
- (2) The effect of random motions on estimated distances.
- (3) Sampling bias connected with fiber collisions.
- (4) Distortion of tessellation cells near edges of the data space.
- (5) The initial random field of density perturbations.
- (6) The finite number of galaxies forming randomly in the evolving density field.
- (7) Sampling a small subset of the galaxies that have formed in the given volume.
- (8) The variety of distinct but equally justifiable definitions of structures.
- (9) The variety of different analysis methods.
- (10) The variety of different selections of input data.

Many of these items are either noise (to be removed, diminished, or otherwise accounted for) or signal, depending on the context. The following discussion addresses this distinction, for the listed items, as dictated by our goals. The direct observational errors in (1) are described in (Blanton et al. 2005; Abazajian et al. 2009), and include both small approximately normally distributed errors and larger outliers. In a nutshell the sky-positional errors are quite small on the scale of interest here, and the random distance uncertainties derived from redshift errors are on average much less than  $\approx 0.5$  Mpc. Here we do not try to remove redshift distortions (2), reserving their treatment to post-factor examination of the shapes of dense clusters. The sampling bias issues connected with fiber collisions (3) and Voronoi cells near edges (4) were discussed in Paper I. For the present purposes all of these errors can be assumed to be small in magnitude and, due to the inclusion of many individual galaxies, should not substantially impact the overall results.

---

of biomass in a treetop, you have to choose a window of maybe a cubic foot. Ten times less and you sample either a single leaf or a blob of air. Ten times more and you have almost reduced the tree to an operational point.” (Koenderink 1990). Tessellation turns this dilemma on its head: the data points adaptively fix both the size and location of the windows.

The remaining entries in the above list require more discussion. Some are part of the astrophysical signal of interest. A large amount of research has been devoted to issues of uncertainty in computational topology (Edelsbrunner & Harer 2010) and topological data analysis (Zomorodian 2005). This work has focused on simplifications realized by discarding or consolidating less important features yielded by various analysis schemes. Examples of goals of this approach are amelioration of noise, especially *discreteness noise*; reduction of complexity and memory requirements; and promotion of better visualization and understanding of structure revealed by removing extraneous details. This methodology requires quantification of importance, ideas for which range from simple size criteria to the rather complex notions of *topological persistence* (Edelsbrunner 1987; Edelsbrunner et al. 2002; Gyulassy & Natarajan 2005; Edelsbrunner & Harer 2010; Gerber et al. 2010; Carlsson 2013; Chen et al. 2013). Persistence methods postulate that the importance of a feature is measured by how long it is present as some parameter is scanned over a range of values. A quantitative link from persistence to probability may be obtained using bootstrap methods (Marzban & Yurtsever 2011; Chazal et al. 2014; Fasy et al. 2014). More recently the persistence concept has made its way into astronomical applications (Sousbie 2011; Sousbie et al. 2011; Sousbie 2013; Cisewski et al. 2005) resulting in use of the term *the persistent cosmic web*.

However, with our goal of characterizing the complete range of multi-scale structure these methods discard some of the very information we seek. Modern cosmology posits that structure in the Universe started as spatially random density fluctuations. Our Universe evolved deterministically from this single set of initial conditions; this process involves nothing like an ensemble of realizations of a random process (as in errors of observation). Accordingly we consider items (5) and (6) signal, not noise. However in other contexts, such as dark matter simulations, discarding small structures as unimportant consequences of initial spatial randomness may be useful. Item (7), sometimes called *discreteness noise*, is inherent to data consisting of a limited number of points drawn from an unknown distribution. Appendix B of Liivamägi, Tempel & Saar (2012) gives a detailed error analysis of this concept based on the Poisson model of Peebles (1980). But for reasons similar to those discussed with regard to (5) and (6), we also regard (7) as part of the astrophysical signal of interest. (Nevertheless the random Poisson data we have included may be of use in other contexts where noise abatement may be useful.) Our Appendix B contains some further remarks about potential effects of what is often called topological noise.

While any of these last three factors, (5)-(7), are possible justifications for simplification using topological persistence or related measures, neither is actually a source of uncertainty about the reality and nature of multi-scale structure in the current Universe derived from a given redshift survey. The distribution of structures derived from discrete samples provides information about initial fluctuations and their subsequent evolution. Therefore removing or smoothing away small scale structures is at worst discarding useful cosmological information; at best it makes the conclusions dependent on postulated models for the relevant physical processes. For this reason, and because the goal here includes geometrical and not just topological analysis, we do not employ any of the simplification procedures cited above. But in other contexts such as global analysis (e.g.



estimation of a few summary topological statistics, such as genus, Minkowski functionals, or Betti numbers) it may be reasonable to regard scatter about a smooth correlation function or within realizations from different initial data as noise. In such cases countermeasures such as topological persistence techniques may be justified.

The largest source of ambiguity in multi-scale structure is the strong dependence of analysis results on analysis methodology, and the fact that there is no one correct methodology or definition of structures – cf. items (8)-(10). For example, we saw that by merely adjusting the halting criterion for assembling Delaunay tetrahedra into voids (Section 3.2), the output of voids ranges from a single void encompassing the entire space (cf. Figure 3) to a void for each tetrahedron. The question is not where between these extremes the truth lies but what representations provide the most useful information – for example in the comparison of observations and simulations. Better yet, it can be very fruitful to study structural representation as a function of methodological assumptions and values of parameters of the analysis.

The HOP results that follow are examples of convenient representations using a simple notion of *attaching to an elementary structure the neighbors that it dominates* – as in the definitions of Voronoi cells, Bayesian blocks, and groups of building blocks that thread this paper. While a fairly natural construct, this is by no means claimed to be better or more fundamental than any others.

### 3.4. Structures Obtained with the HOP Algorithm

Now turn to some examples of the identification of spatial structures using the HOP algorithm to assemble the elementary *objects* or building blocks (i.e. Voronoi cells, Bayesian Blocks or Delaunay Tetrahedra) into a unique set of connected structures. Each such structure descends or ascends monotonically from one of the *critical objects* – local maxima or minima of the adopted density or voidness function. These peaks – for example each Bayesian block denser than all its face-adjacent neighbors – can be easily identified by direct search but are also automatically produced by the HOP algorithm. The structures attached to the peaks are analogous to their watersheds. Such structures could be classified in one way or another (e.g. in the four customary classes: clusters, filaments, sheets and voids, macroscopically of dimensionality 0, 1, 2 and 3 respectively) but their shapes are widely distributed in shape-space and they do not fit cleanly in discrete clusters of shape parameters.

The sole information needed for each galaxy consists of two items, the first being the value of *the HOP function*  $\mathbf{f}$  – typically a density estimate or its surrogate. It is natural for tessellation-based studies to take as the density of an object the number of galaxies in it divided by its volume. The reasoning for individual Voronoi cells is straightforward: small cells occur in crowded regions where the cell size is small. This relation intuitively supports the idea that the reciprocal of a cell volume is a reasonable surrogate for local density at or near that cell. In addition this construct can provide an unbiased estimate of local density (Platen et al. 2011). The fact that only the relative

order of the densities matters (item 7 in the list of properties of HOP in Section 3.1) is further protection against bias effects. Correspondingly the density we assign in the case of Bayesian Blocks is the number of galaxies in the block divided by its volume, the latter defined as the sum of the volumes of the cells making up the block. In the KDE case we evaluate the estimated continuous density field at the position of each galaxy. One of the SOM parameters is taken as a rough density surrogate (Paper I).

The other item necessary is a list of adjacent neighbors for each galaxy. As indicated earlier in Section 3.1 for the Voronoi-based tessellations, we take two objects  $A$  and  $B$  (cells or blocks) to be adjacent to each other if and only if there is at least one pair of Voronoi cells, one member of the pair in  $A$  and the other in  $B$ , which share a common face. Here we take advantage of the natural definition of a data-adaptive number of near neighbors that Voronoi tessellation provides. The KDE algorithm does not determine neighbors, and we simply impose the adjacency information copied from the Voronoi tessellation. Two Delaunay tetrahedra are considered adjacent if and only if they share a common triangular face.

Note that Voronoi cell volume is not a property of a single galaxy but is determined by its propinquity to its neighbors; hence information from distances to other galaxies is represented in both the cell volumes and the identities of neighboring cells.

Table 1 summarizes for the SDSS data some of the basic properties of the collections of structures resulting from five choices for the building blocks for structures. In higher dimensional Bayesian blocks (Jackson et al. 2010) one constructs a 1D array consisting of ordered values of a cell variable. In Paper I this quantity was taken to be the volume of the Voronoi cell. Since HOP more naturally operates on density we also redid the whole Bayesian Block analysis of Paper I, this time using density as the cell variable instead of volume. These two analyses are listed in the first two rows of the table, showing that there is not a large difference in the number of structures identified. The nature of the HOP input for the other 3 cases are described by the corresponding entries in the first two columns of the table. The second column indicates the definition of  $\mathbf{f}$ , taken to be the density of galaxies within a Bayesian Block or Voronoi cell, KDE density, or SOM class. The objects fed to the HOP algorithm (Column 1) are individual galaxies except in the first two cases, where they are collections of galaxies in blocks. The third column indicates the number of objects input to the algorithm. The last two columns give the number of structures, or groups of galaxies, associated with density maxima and minima.

The following two tables record similar information for the other two data sets, the Millennium Simulation, and independently and randomly distributed points, respectively.

For a representative selection of the cases in Tables 1, 2, and 3 Figure 4 plots normalized distributions of the structures' effective radii, defined in terms of its volume  $V$  by

$$R_{\text{eff}} = H_0 (3V/4\pi)^{1/3} , \tag{1}$$

Here for  $V$  we use the sum of the volumes of the Delaunay tetrahedra in the structure, but al-

Table 1: Statistical Summary of SDSS Structure Collections.  $V_{block}$  and  $V_{Voronoi}$  are the volumes of the blocks and cells, respectively, and  $N_{gal}$  is the number of galaxies in a block. There are 146,112 galaxies before the fiber collision and edge cuts.

Objects	<b>f</b>	Num. of Objects	Num. of Structures	
			Maxima	Minima
Bayesian Blocks (volume)	$N_{gal}/V_{block}$	41,672	7,517	752
Bayesian Blocks (density)	$N_{gal}/V_{block}$	46,491	11,273	178
Galaxies	KDE	133,991	6,615	1,796
Galaxies	$1/V_{Voronoi}$	133,991	10,414	1,032
Galaxies	SOM class	133,991	2,076	10,516

Table 2: Statistical Summary of MS Structure Collections.  $V_{block}$  and  $V_{Voronoi}$  are the volumes of blocks and cells, respectively, and  $N_{gal}$  is the number of galaxies in the blocks. There are 171,388 galaxies before the fiber collision and edge cuts.

Objects	<b>f</b>	Num. of Objects	Num. of Structures	
			Maxima	Minima
Bayesian Blocks (Volume)	$N_{gal}/V_{block}$	54,850	8,848	1,036
Bayesian Blocks ( $\rho$ )	$N_{gal}/V_{block}$	57,305	12,023	404
Galaxies	KDE	148,927	9,859	9,767
Galaxies	$1/V_{Voronoi}$	148,927	12,618	532
Galaxies	SOM class	148,927	11,603	12,979

Table 3: Statistical Summary of Poisson Structure Collections.  $V_{block}$  and  $V_{Voronoi}$  and  $N_{gal}$  is the number of galaxies in the blocks. There are 144,700 points before the fiber collision and edge cuts.

Objects	<b>f</b>	Num. of Objects	Num. of Structures	
			Maxima	Minima
Bayesian Blocks (Volume)	$N_{gal}/V_{block}$	30,218	6,823	3,090
Bayesian Blocks ( $\rho$ )	$N_{gal}/V_{block}$	42,471	11,009	2,395
Galaxies	KDE	131,832	2,313	2,765
Galaxies	$1/V_{Voronoi}$	131,832	10,009	3,374
Galaxies	SOM class	131,832	8,558	11,522

ternatively one could use the equal or slightly larger volume of the convex hull. The distributions obtained with direct local density estimates (BB, Voronoi and KDE) are similar, with broad peaks in the range 10-20 Mpc. The SOM distributions are based on a HOP function that is discrete and only indirectly expresses density, so it is not surprising that they are rather different from the others. These distributions are quite similar to that shown in Figure 2 of Pan et al. (2012).

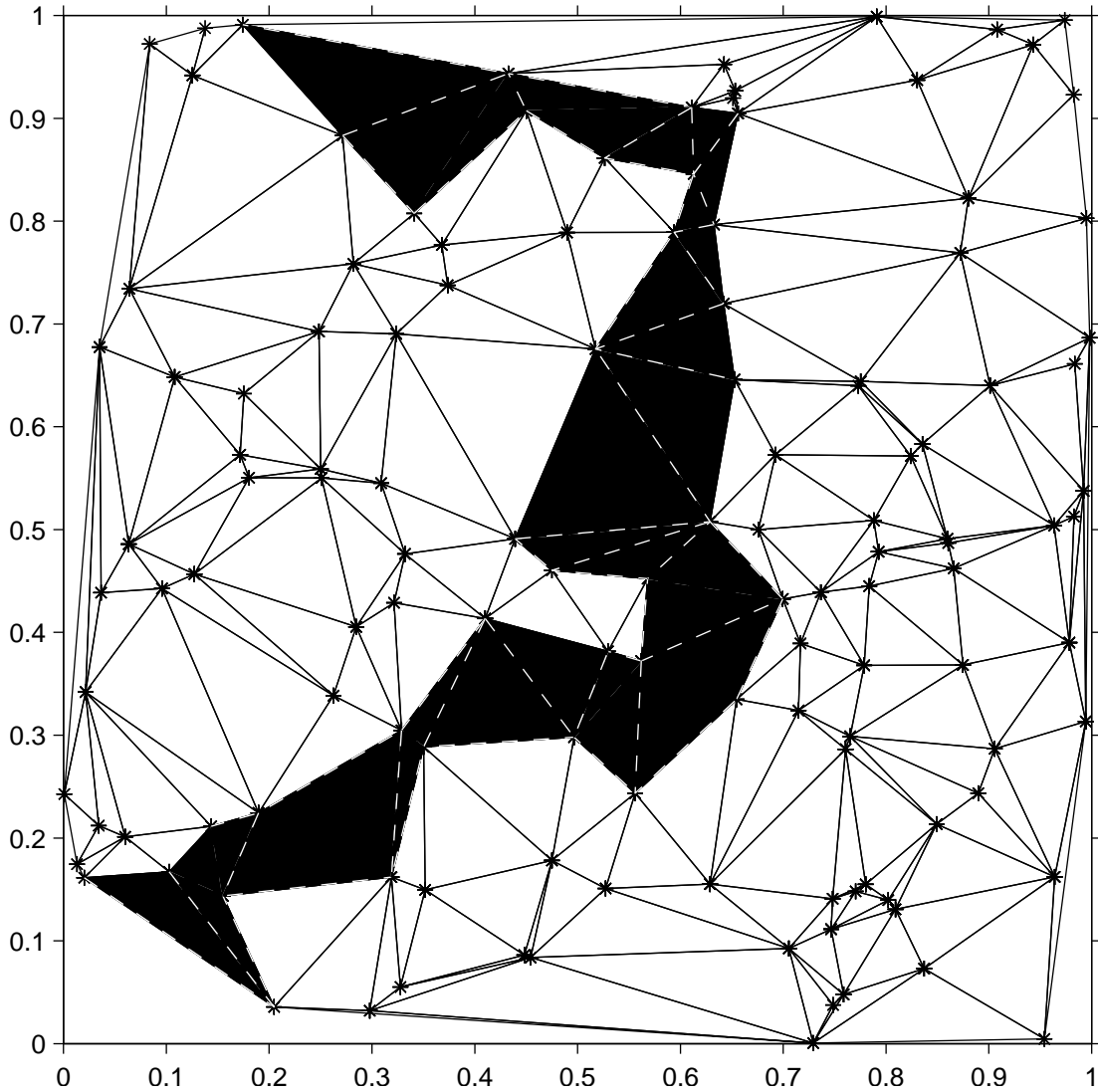


Fig. 3.— Delaunay triangulation of 132 random point in the unit square. The set of shaded triangles comprises a connected region empty of points but with a shape dictated by the rather arbitrary choice of which triangles to paste together.

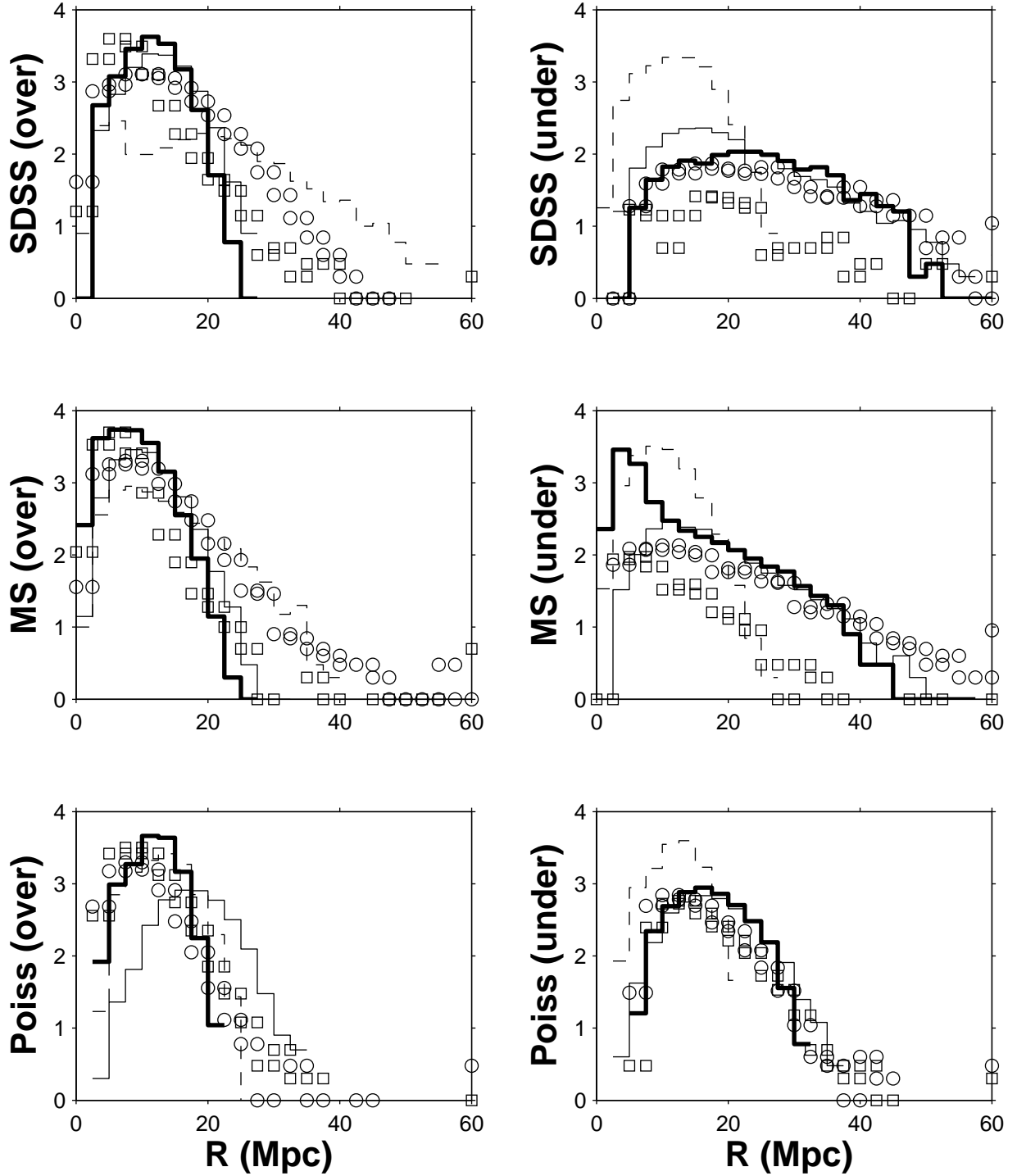


Fig. 4.— Distributions of the effective radii of groups connected with density maxima (left) and density minima (right) found with HOP for the three standard data samples: SDSS (top), MS (middle), and Poisson (bottom). Thick Solid: Voronoi; solid: KDE; dashed: SOM; circles: BB (volume) and squares: BB (density). In each case the base-10 log of the number distribution is plotted against the effective radius in Mpc.

The region of the Sloan Great Wall is perhaps the richest region of the nearby Universe. Figure 5 compares our group structures from Voronoi cells alone (corresponding to row 4 of Table 1 labeled  $1/V_{Voronoi}$ ; colored polygons) with superclusters in this region (crosses inside circles). The bulk of the Sloan Great Wall is in the lower-left quadrant. This figure is limited to galaxies in the redshift range .045 – .085 ascribed to the Great Wall. To eliminate some clutter only HOP groups with 25 or more galaxies and projected areas of more than 16 square degrees are shown. The correspondence with previously cataloged superclusters is not one-to-one, as expected because of the very different detection principles involved.

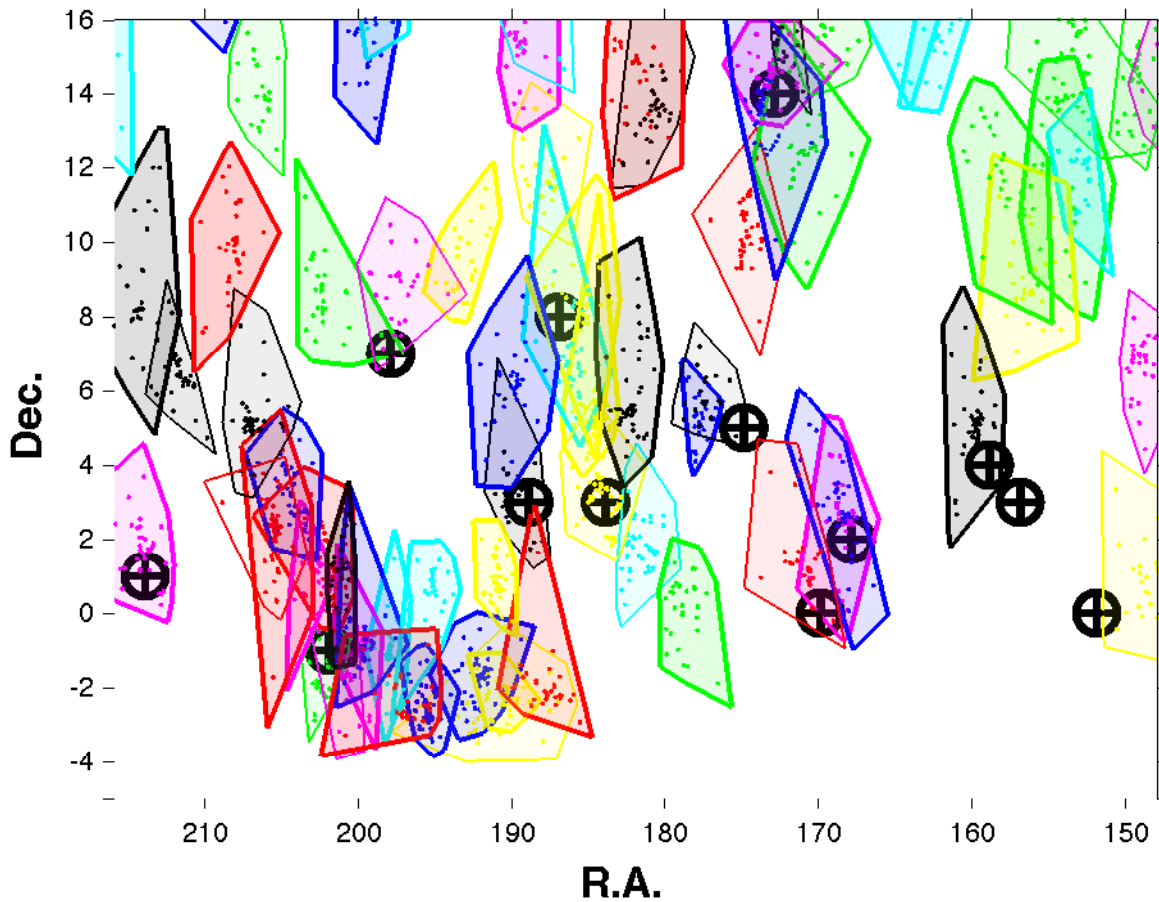


Fig. 5.— Sky distribution of galaxies for the region of the Sloan Great Wall. The HOP groups are delineated by polygons filled with random colors. These are the projected 2D convex hulls of the sky positions of galaxies contained in the group, slightly expanded to improve the visualization. The opacities of the polygons are linear in the redshift for the group: close darker ones thus appearing to be in front of more distant lighter ones. The heavy black circles with + signs are nominal positions of the 13 superclusters in this region given in Table 1 of Einasto et al. (2011).

### 3.5. Some Properties of Delaunay Voids

We now discuss voids in more detail, pointing out some potential problems that need to be addressed, including the possibility of galaxies lying inside Delaunay voids and edges effects similar to those mentioned above and in Paper I for dense structures.

The Delaunay tetrahedron method described above yields volumes almost completely devoid of galaxies in the sample. From the way these void structures are constructed the galaxies at the vertices of the component tetrahedra for the most part lie on the void surface leaving the inside empty. A surface galaxy is one from which there is a path to the outside that does not intersect any of the tetrahedra. With this definition a galaxy is inside a Delaunay void if and only if all of the void’s tetrahedra that have it as a vertex cover the full solid angle ( $4\pi$  steradians) as seen from that galaxy. A simple but effective procedure to identify Delaunay voids and identify possible interior galaxies is as follows:

- Compute the Delaunay tessellation of the galaxy positions
- Identify groups of tetrahedra making up voids using HOP with  $\mathbf{f} = \text{tetrahedral volume}$
- For each such Delaunay void, containing  $N_{void}$  tetrahedra:
  - Collect a list of all  $4N_{void}$  triangular faces of the tetrahedra making up the void
  - Identify the faces that appear in this list only once.
  - The vertices of such faces are on the surface.
- Identify as internal galaxies any that are not on the surface

In summary we define surface galaxies as those that populate the hull (not to be confused with the convex hull) of the galaxies circumscribing the void; any void galaxies not on the hull are then internal. In our analyses this is not an issue: *not a single one of the many HOP-found Delaunay voids reported here contains any internal galaxies.* Clearly our analysis method militates strongly against such cases, but we do not know if they are impossible or just extremely rare.

While edge effects in Delaunay tessellations are less serious than in Voronoi tessellations, a second potential problem is that tetrahedra at the edges of the data space are systematically larger than they would be if not located there. Due to the complexity of the SDSS boundaries in three dimensions an automated test for whether or not a tetrahedron is at or near an edge is difficult. Here we compute the minimum distance of the four galaxies in a tetrahedron from the nearest point on the convex hull of the data. A complication arises when the outward-facing triangles of tetrahedra at the edge are exceptionally large, for then this minimum inter-galaxy distance is not actually representative of the distance from the edge. This difficulty is easily circumvented by adding points just outside these triangles, thus creating an augmented convex hull, faithful to the actual one but with no large faces. Figure 6 gives scatter plots of effective radius vs. distance



from the augmented hull, clearly showing this inflation effect for voids within approximately .005 redshift units of the hull.

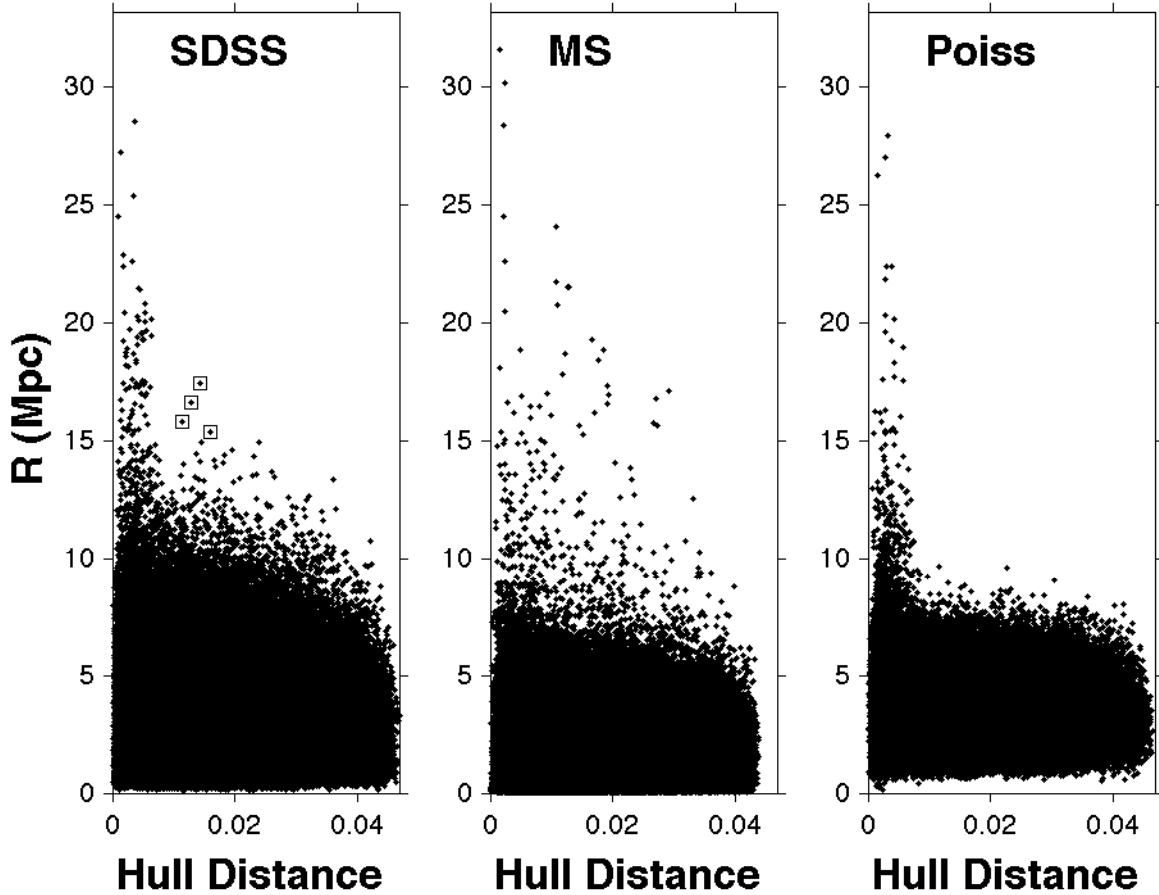


Fig. 6.— The effective radius of each Delaunay void is plotted against the minimum distance from its circumscribing galaxies to vertices of the augmented convex hull of the full data set. In all 3 cases (SDSS: left, MS: middle, Poiss: right) the sprinkling of large-radius voids at small distances from the hull are artificially enlarged due to edge effects.

Figure 7 shows 3D plots of the four largest SDSS voids that are farther than .007 redshift units from the augmented hull (indicated by squares drawn around the points in Fig. 6 above). The largest of these voids (upper left panel) is centered at  $RA = 14.5 \pm 0.2^h$ ,  $DEC = 39.4 \pm 2.2^\circ$ , and  $z = 0.1041 \pm .0034$ , and is therefore near and possibly associated with the so-called *Boötes* or *giant void*, given various positions by different authors – e.g.  $RA \approx 13^h$  [11.5 - 14.3],  $DEC \approx 40^\circ$  [26.5 - 52.0], and  $z \approx 0.11$  by Kopylov & Kopylova (2002). There is a very different kind of structure, an order of magnitude larger in linear size and containing, according to these authors, not just galaxies but 17 clusters in the ranges shown. It is clear that we are finding very different void structures than those obtained with other methods.

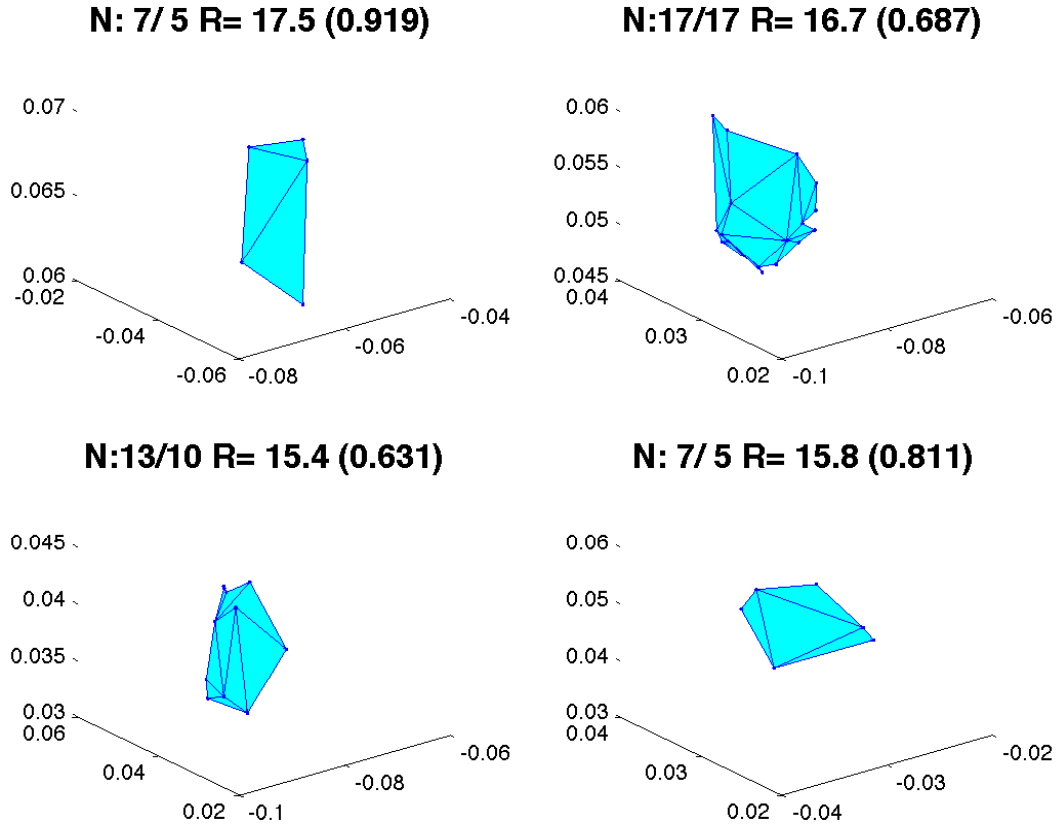


Fig. 7.— The four largest SDSS Delaunay voids judged to be free of edge effects, and indicated with squares in the upper-left panel of Fig. 6. The two integers in the legends are the number of circumscribing galaxies and tetrahedra, respectively – followed by the effective radius in Mpc and in parentheses the convexity (the sum of volumes of the tetrahedra divided by the volume of the convex hull of the galaxies).

Voids are typically considered to be regions where the density of galaxies is  $\approx 10\%$  of the mean density and 10's of megaparsecs in size (e.g. Pan et al. 2012; Coil 2012; Patiri et al. 2013). By definition the Delaunay voids derived here have no galaxies within the analyzed data set and hence have close to 0% of the mean density.

Figure 8 gives some insight on the information about densities implied by our empty voids. If the number of galaxies in a given volume follows the Poisson distribution, the likelihood  $P(\lambda) = e^{-\lambda V}$  for the rate  $\lambda$  (galaxies per unit volume) in an empty volume  $V$  gives an upper limit of  $\lambda_{ul} = -\log(p_0)/V$  with a confidence of  $1 - p_0$ . The figure plots the distribution of this quantity for  $p_0 = 0.05$  (equivalent to a 95% confidence). In order to avoid cells with inflated volumes due to edge effects a cut of .0055 redshift units (205 Mpc) was applied on the minimum distance between

the void vertices and the nearest face of the convex hull of the full data set. In addition most of the large number of upper limits larger than the overall mean density (shown as a vertical dashed lines) are simply not shown. These are not rigorous upper limits, and the only point is that the SDSS and MS samples yields a number of voids with lower limits considerably smaller than 10 percent of the mean density and somewhat lower than the random sample. Further density information about the voids detected may come from a census of SDSS galaxies not included in our volume limited (VL) sample. Some of those not included in the VL sample will contain spectroscopic redshifts to the limit of the Main-Like galaxy sample ( $m_r < 18$ ) (cf. Section 5.3) while others may contain photometric redshifts to the limit of the photometric sample ( $m_r < 21$ ) (see, York et al. 2000; Strauss et al. 2002). A future paper will explore density limits in voids, as well as other descriptors of structures.

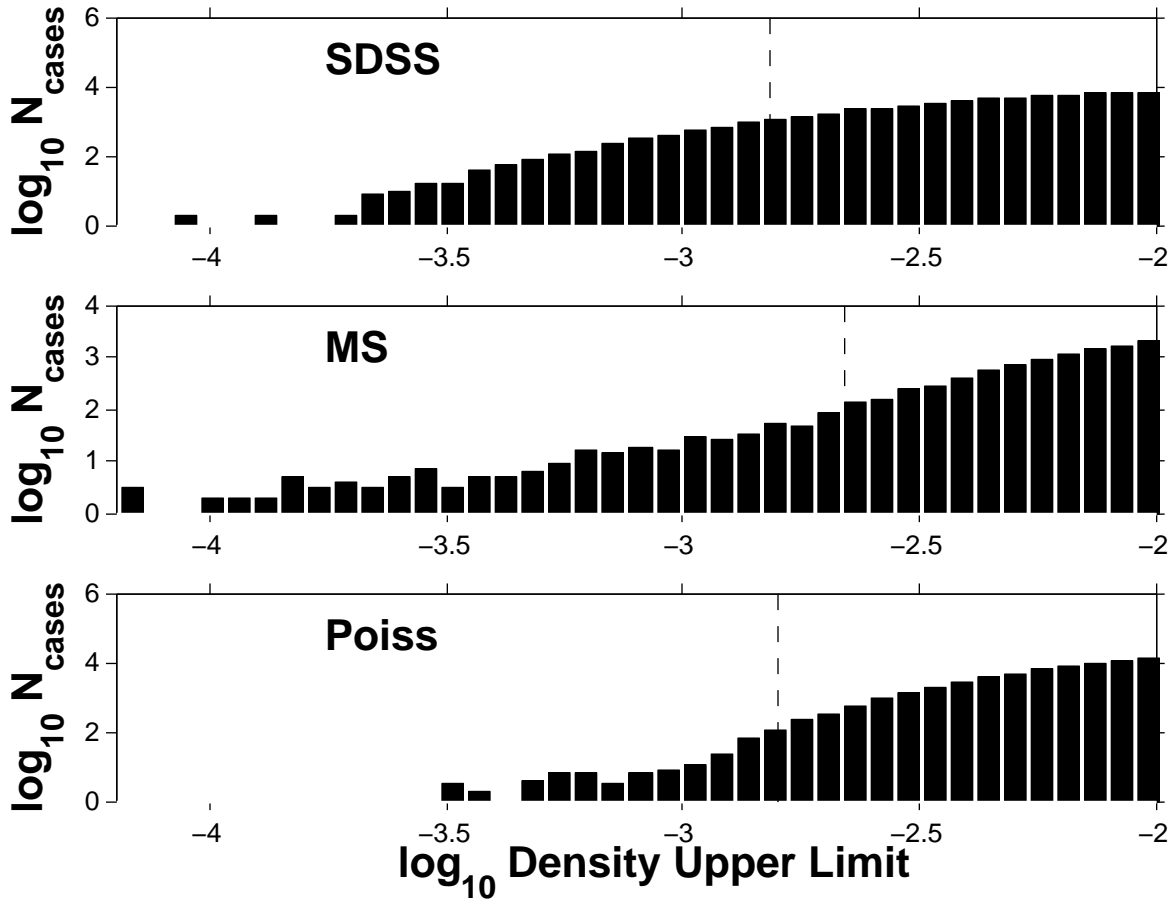


Fig. 8.— Distribution of upper limits (galaxies per cubic Mpc) implied by the emptiness of Delaunay voids.

## 4. Conclusions

We have provided tools and data products to explore the multi-scale structure of the distribution of galaxies, using the SDSS DR7 redshift survey data, and in comparison to simulated and random data. The procedure demonstrated here departs from other work in use in several ways. Starting with structural building blocks in the form of tessellation elements or small collections of them, we use the HOP algorithm to identify structures connected with density maxima and minima, using the density estimators described in Paper I for the HOP function, coupled with adjacencies defined by Voronoi-Delaunay tessellation. Our HOP-based procedure is much simpler than those based directly on discrete Morse theory. Nevertheless it identifies all local density maxima and minima plus their descending and ascending manifolds. Furthermore we eschew methods such as topological persistence because, by eliminating structures based on a notion of importance, they unnecessarily discard valuable information. Such methods may allow one to concentrate on certain salient features, but the results are then dependent on the choices of *importance quantifier* and methods for discarding, combining or otherwise modifying features.

Note that Nature does not single out any one definition of structural elements or procedures for identifying and characterizing them. Methods invoking other than the purely geometrical information utilized here, such as colors or gravitational binding, undoubtedly yield very different structural descriptions. This dependence on methodology is not an uncertainty, statistical or otherwise, but an inevitable and useful feature of the diversity of analysis approaches.

A few summary statistics are presented here and further details will be presented in future publications. Three dimensional distributions of multi-scale structure are not easily displayed in a paper. We encourage the reader to explore visualizations of the data given as electronic-only material. Such displays might be compared to the density map shown in Figure 2 of Gott et al. (2008) which suggests a visual similarity of the distribution of the highest 7% and lowest 7% of a smoothed and pixelated density distribution. Such displays of course cannot convey a complete visualization, rather they show that these two spatial distributions of very different quantities (one of galactic density, the other of degree of local sparsity) are at least superficially quite similar. A future paper will explore this similarity by investigating auto-correlation functions, cross-correlation functions, and other statistical techniques, and make detailed comparison with similar collections of multi-scale results such as dense structures (Park et al. 2012) and voids (Sutter et al. 2012).

All of the data needed to construct structure catalogs are contained in electronic-only files described fully in Appendix A. We provide files containing information to construct catalogs of multi-scale density and void structures based on several modes of analysis of the data, with a special eye toward comparing SDSS structures with those in simulation and purely random data sets. Each galaxy is assigned to a structure defined by a local maxima, and the collection of these for a given maximum define a max-structure (also called a group or cluster). In addition each galaxy is also assigned to a structure defined by a local minimum, with the collections defining min-structures (or voids). One can apply cutoffs in order to limit the outskirts of individual structures, procedures

to eliminate structures that are not significant according to a given criterion, and possibly other post processing techniques.

The geometrical structures in the spatial distribution of galaxies, here termed *the multi-scale structure of the Universe*, have been said to form a *hierarchy* (van de Weygaert et al. 2009; Neyrinck 2008; Aragon-Calvo et al. 2010b; Aragon-Calvo & Szalay 2013), often without a precise definition of what this means. This nomenclature implies the existence of a set of *discrete* hierarchically related levels. These ideas seem to be derived from concepts such as merger trees in theoretical or phenomenological models of structure formation; cf. the discussion in Knebe et al. (2013). It is possible that signatures of such effects can be detected in the current multi-scale structure, say in the form of clusters of clusters of galaxies (popularly referred to as superclusters) and the like (but see Yu & Peebles 1969). However studies of characteristics of multi-scale structure in the universe, including the present work, demonstrate only continuous distributions and fail to show evidence of discreteness in either qualitative characteristics or quantitative observables. A continuous or self-similar distribution (e.g. Einasto et al. 1989) is if anything the opposite of a discrete hierarchy. A similar point has been made by Peebles (1974, 1984). In short we see no evidence of a discrete hierarchy in the multi-scale structure of the Universe. Note that the discrete density levels of Bayesian Blocks or Kernel Density Estimation described here and in Paper I are a contrivance for density representation and have nothing to do with a discrete hierarchy of any kind in the actual distributions.

The catalogs and other data products given here can be utilized by any group to compare the structures found by any technique and make them immediately comparable to those of another. Future papers in the current series will describe more detailed statistical summaries of geometric and topological properties of both over-dense, under-dense, and empty structures, and carry out various comparisons with previous cluster and void catalogs.

We are grateful to the NASA-Ames Director’s Discretionary Fund and to Joe Bredekamp and the NASA Applied Information Systems Research Program for support and encouragement. Thanks goes to Ani Thakar and Maria Nieto-Santisteban for their help with our many SDSS casjobs queries. Michael Blanton’s help with using his SDSS NYU–VAGC catalog is also very much appreciated. We are grateful to Patrick Moran, Christopher Henze, Changbom Park, Paul Sutter, Mark Neyrinck, Thierry Sousbie, Tom Abel, Pratyush Pranav, Peer-Timo Bremer, Attila Gyulassy, James (“B.J.”) Bjorken and Jessi Cisewski. Special thanks goes to Slobodan Simic and members of the CAMCOS project at San Jose State University, Joseph Fitch, David Goulette, Jian-Long Liu, Mathew Litrus, Brandon Morrison, Hai Nguyen Au, and Catherine (Boersma) Parayil for useful comments and for an ongoing collaboration on developments of the HOP algorithm for topological data analysis. None of these acknowledgements should be construed to imply agreement with the ideas expressed here.

Funding for the SDSS has been provided by the Alfred P. Sloan Foundation, the Participating Institutions, the National Aeronautics and Space Administration, the National Science Foundation,

the U.S. Department of Energy, the Japanese Monbukagakusho, and the Max Planck Society. The SDSS Web site is <http://www.sdss.org/>.

The SDSS is managed by the Astrophysical Research Consortium for the Participating Institutions. The Participating Institutions are The University of Chicago, Fermilab, the Institute for Advanced Study, the Japan Participation Group, The Johns Hopkins University, Los Alamos National Laboratory, the Max-Planck-Institute for Astronomy, the Max-Planck-Institute for Astrophysics, New Mexico State University, University of Pittsburgh, Princeton University, the United States Naval Observatory, and the University of Washington.

This research has made use of NASA's Astrophysics Data System Bibliographic Services. This research has also utilized the viewpoints (Gazis et al. 2010) software package.

## 5. Appendix A: Data Details

Of the three data sets studied, the first is a volume limited sample of 146,112 galaxies drawn from the SDSS. The second catalog is drawn as similarly as possible from the MS, yielding a volume limited sample of 171,388 galaxies. Third is a set of 144,700 points mimicking the SDSS volume limited sample but randomly and independently distributed so that there is no spatial structure beyond that imposed by the SDSS sampling.<sup>11</sup> All conversions from redshift coordinates to Mpc are based on a Hubble constant of  $73 \text{ km s}^{-1} \text{ Mpc}^{-1}$ .

### 5.1. The SDSS NASA/AMES Value Added Galaxy Catalog (AMES-VAGC)

This section provides details in addition to those given in Paper I. The NASA/Ames Research Center SDSS Value Added Catalog (NASA-AMES-VAGC) is based on the New York University Value Added Catalog (NYU-VAGC Blanton et al. 2005), that is in turn derived from Data Release 7 of the SDSS (Abazajian et al. 2009). We now describe the stages in the catalog creation.

### 5.2. Stage 1: Extracting tables from the SDSS NYU-VAGC

The contents of a number of NYU-VAGC fits table files (described below) were extracted and used to create *Stage 1* of the catalog. An index of those fits files is listed below. At the time the catalog was created only the NYU-VAGC had SDSS K-corrected absolute magnitudes readily available and hence we did not originally use the catalogs available via the excellent SDSS casjobs server.<sup>12</sup>

Selections were applied to each of the following three NYU-VAGC fits files:

- object\_sdss\_spectro.fits:
  - SDSS\_SPECTRO\_TAG: Galaxy Spectrum exists
  - PRIMTARGET: Select Main Galaxy Sample targets
  - OBJTYPE: Select type GALAXY
  - CLASS: Select type GALAXY
  - Z: Estimated redshift
  - Z\_ERR: Estimated redshift error. Only allowed to be greater than zero since negative values indicated an invalid estimate

---

<sup>11</sup>Such identically and independently distributed (IID) processes are often called Poisson processes (here with a spatially constant event rate) because the counts in fixed volumes obey the Poisson distribution.

<sup>12</sup><http://casjobs.sdss.org>

- ZWARNING: Must be equal to zero to indicate no warning flags in the redshift estimation procedures
- object\_sdss\_imaging.fits:
  - RA: Right Ascension
  - DEC: Declination
  - NCHILD: Must be zero indicating that it is not part of a blended parent or blended itself (!BLENDED)
  - RESOLVE\_STATUS: Used to obtain only one instance of each object
  - VAGC\_SELECT: To satisfy the Main-like criteria of the NYU–VAGC
  - FLAGS: Include only !BRIGHT, !BLENDED, !SATURATED
  - MODELFLUX: Model Magnitude fluxes (extinction corrected)
  - MODELFLUX\_IVAR: Inverse variance of the fluxes (flux errors)
  - PETROR50: 50% Petrosian Radius
  - PETROR90: 90% Petrosian Radius
- kcorrect.none.model.z0.10.fits:
  - ABSMAGS: Absolute magnitudes in U,G,R,I,Z,J,H,K using a 0.1 blue-shift of the bandpasses for k-corrections

The outputs of these selections were concatenated into a single *Stage 1* NYU–VAGC Main–Like Galaxy Sample catalog containing 561,421 galaxies. See Figure 9 for a plot of the points in Right Ascension (RA) and Declination (DEC). The catalog at this stage contained an internally assigned identification number, RA, DEC, apparent magnitudes (u,g,r,i,z), apparent magnitude errors, absolute magnitudes (U,G,R,I,Z,J,H,K), absolute magnitude errors, redshift, redshift error, Petrosian 50% and 90% radii.

### 5.3. Stage 2: Obtaining a contiguous and volume limited sample

The maximum number of galaxies in our volume limited sample consistent with common practices in using the SDSS turned out to be 163,157. These selections (e.g. Choi et al. 2010) are redshift  $z < 0.12$ , absolute magnitude in the r bandpass  $M_R^{0.1} < 20.0751$ . These are consistent with a red band apparent magnitude upper limit defined by the Strauss et al. (2002) Main Galaxy Sample as  $r < 17.77$ , although the NYU–VAGC Main-like sample goes down to  $r = 18$ .

Next samples were removed outside a defined contiguous region avoiding several irregular features extending beyond the smooth outer (two dimensional) shape of the distribution of points,



as well as disconnected and isolated patches lying entirely outside. This region was centered on the north galactic cap roughly corresponding to  $100 < \text{RA} < 270$  and  $-7 < \text{DEC} < 65$ . The contiguous region contains 146,112 objects and is defined by the gray area in Figure 9.

#### 5.4. Stage 3: 55'' fiber placement issue and coordinate transform

The angular separation in arc-seconds to the 6 nearest neighbors for every point was estimated. This allows one to quickly identify any neighbor within 55''. This was necessary because the fiber plug plate of the SDSS does not allow fibers to be placed closer than 55'' to each other. However, there are a large number of overlapping plates which means that there are some galaxies with spectra within this 55'' fiber limit. Since these overlaps cover only part of the full area it represents a systematic bias that must be eliminated in order to consistently sample the true underlying galaxy distribution. To do so we removed a randomly chosen member of any pair found within 55'' of each other. This process eliminates 6,314 galaxies from the sample.<sup>13</sup>

To use Euclidean coordinates with units the same in all 3 dimensions the right ascension ( $\alpha$ ), declination ( $\delta$ ), and redshift ( $z$ ) were transformed into Cartesian coordinates according to

$$x = z \cos(\delta) \cos(\alpha) \tag{2}$$

$$y = z \cos(\delta) \sin(\alpha) \tag{3}$$

$$z = z \sin(\delta) \tag{4}$$

(equivalent to the MatLab© function `sph2cart`) thus yielding rectangular coordinates, each with units of redshift and convertible to physical units by multiplying by  $c/H_0$ , with  $c$  the speed of light and  $H_0$  the Hubble constant. A nonlinear conversion can also be made for a given cosmological model, but will yield only a small correction over the low redshift range of these data.

#### 5.5. Stage 4: Voronoi related calculations

The Voronoi tessellation (e.g. Okabe et al. 2000) of the remaining galaxies was calculated (see Paper I for more details). From this tessellation a number of additional parameters are derived:

1. Cell volume:  $V$
2. The distance between each galaxy and the center of its Voronoi cell:  $d_{CM}$
3. The minimum and maximum dimension of each Voronoi cell:  $R_{min}, R_{max}$

---

<sup>13</sup>In Paper I it was claimed that 6,540 galaxies were eliminated, but this is incorrect.

4. Cell radius:  $R_{Voronoi} = (\frac{3V}{4\pi})^{1/3}$
5. A measure of cell elongation:  $E = \frac{R_{min}}{R_{max}}$
6. A measure of the magnitude of the local density gradient:  $d_{CM}/R_{Voronoi}$
7. A scaling parameter for distances: the average density of the volume limited SDSS data raised to the minus 1/3 power:  $d_{uniform} = 3.2 \times 10^{-3}$  in units of redshift

The first three are fundamental properties of the Voronoi cells. They are defined for individual cells but are dependent on neighboring galaxies by virtue of the way the Voronoi tessellation is defined. In turn they are used to derive useful properties 4, 5 and 6. The first two of these are summary descriptions of the size and shape of the cell. The separation between each galaxy and the center of its Voronoi cell is a vector that approximates the magnitude and direction of the local gradient in the density of galaxies. It is here represented by its magnitude in item 6.

The average distance in item 7, a property of the full sets of galaxies in the catalogs, is not used in the assignment of individual galaxies to classes. Instead, it is used as a scaling factor to make distance parameters such as  $d_{CM}$  and  $R_{Voronoi}$  dimensionless. The average distance here is computed as the average spacing,  $(V/N)^{1/3}$ , between samples. The actual value for the Millennium simulation was very near that of the SDSS, while the Random was set to this value when the data set was created. This quantity was chosen because it is well-defined, straightforward to calculate, and insensitive to details such as the usage of the Voronoi tessellation algorithm.

### 5.6. Stage 5: Flagging boundary points

The cells near the boundaries of the tessellated volume are distorted to one degree or another. Depending on the distance of the cell from the boundary, this effect ranges in importance from small to large. The most distortion happens when the tessellation algorithm assigns to a cell one or more vertices well outside the data volume, or even leaves a vertex undefined because it formally lies at infinity. One could attempt to correct for such distortion but as described in Paper I we feel it is better to simply eliminate galaxies whose Voronoi cells appear to have been significantly distorted by boundary effects. Our criteria for identifying such cells, as detailed in the Section titled “The Voronoi Cell Boundary Problem” of Paper I, led to the rejection of 5807 boundary cells, leaving 133,991 galaxies in the sample to be used for the SDSS density estimations reported here.

### 5.7. Stage 6: Building a table for casjobs

In order to make the sample useful for users of casjobs (where most SDSS users obtain their data) we have attempted to obtain SDSS object identification numbers from the PhotoOb-

jAll.ObjID table for all of the objects in the final density sample. This was necessary because the NYU–VAGC DR7 catalog does not contain the same object identification numbers as those found in the SDSS DR7 casjobs catalog. To obtain the object identifications the fGetNearestObjAllEq function of casjobs was used. Objects were matched within 1'' of the RA and DEC of the NYU–VAGC derived objects.<sup>14</sup> From 146,112 points (see Section 3.2) 145,875 PhotoObjAll.ObjID identifications were found (known simply as the ObjID in SDSS casjobs parlance), meaning that 237 points did not exist in the casjobs catalog. This 0.16% loss should not be a major inconvenience for casjobs-based procedures. Those 237 objects in the final NASA–AMES–VAGC catalog without casjobs ObjID numbers will still be in the publically released catalog, but will instead contain an 18 character string (the same length as the unique SDSS ObjID) with each object numbered from 00000000000000000001 to 00000000000000000237.

### 5.8. The adaptive kernel map classes

In Table 3 of Paper I the Bayesian Blocks (BB) and adaptive kernel map (AKM) methods had a number of classes that ranged from low density to high. The class structure for the Self Organizing Map (SOM) method was more complex (see Table 2 in Paper I). The AKM method produces a continuous range of densities rather than specific classes. In order to mimic the BB and SOM class methods a filter was applied to the AKM densities to produce the 11 classes found in Table 3 of Paper I:

$$AKM_{class} = 12 - \text{round}(((\log_{10}(AKM_{density})/5.6947) \times 20) - 7) \quad (5)$$

Fig. 10 shows the resulting correspondence between AKM density and class.<sup>15</sup>

### 5.9. The Millennium Simulation AMES Value Added Catalog

To create a volume limited sample from the MS a similar procedure was followed to that described in Section 5.1. This is possible since one can obtain the absolute magnitude estimates in the same bandpasses as the SDSS for the galaxies in the MS (Croton et al. 2005). First one must convert the MS Cartesian coordinates and velocities ( $x, y, z, v_x, v_y, v_z$ ) to right ascension, declination, and redshift using  $H_o=73 \text{ km sec}^{-1} \text{ Mpc}^{-1}$ ,  $\Omega_M=.25$ ,  $\Omega_\Lambda=.75$ ,  $\Omega_K=0$ . The apparent magnitudes were derived from the given absolute magnitudes using the luminosity distance. The luminosity

---

<sup>14</sup>Query: select a.\*, b.objid as matchObjID into mydb.nyuvagccross from MyDB.densitycatalog a cross apply dbo.fGetNearestObjAllEq(a.ra, a.dec, 0.0167) b

<sup>15</sup>A better method to segment the data might have been to utilize the unique strengths of Bayesian Blocks, but that was not done herein.

distance requires the redshift and radial distances derived from the MS.<sup>16</sup> The same redshift, absolute magnitude cuts as in the AMES–VAGC were applied leaving 171,388 out of  $\sim 9$  million points in the original MS catalog. 16,283 points were eliminated to emulate the SDSS 55'' fiber collision issue, while 6178 were eliminated because of boundary effects. This leaves 148,927 points.

The same distance scaling factor as used for the SDSS data, as described in Section 5.5, Item 7, namely  $d_{uniform} = 3.2 \times 10^{-3}$ , was used to derive the same Voronoi quantities found for the SDSS in Section 5.5.

Again, in order to mimic the BB and SOM class methods a filter was applied to the AKM densities to produce the 13 MS classes found in Table 3 of Paper I:

$$AKM_{class} = 14 - \text{round}(((\log_{10}(AKM_{density})/5.6947) \times 20) - 7) \quad (6)$$

### 5.10. The Randomly Distributed Point Catalog

The creation of the randomly distributed data point catalog was outlined in detail in Paper I. The initial data set contains a similar number of points (144,700) as both the AMES–VAGC and derived MS catalogs. The final catalog, after removing 6219 points corresponding to the 55'' issue discussed previously and 6649 boundary points discovered after the Voronoi tessellation yields 131,832 points.<sup>17</sup>

The galaxy positions were then converted to rectangular Cartesian coordinates according to the same formulas used for the SDSS data, namely eqs. (2), (3) and (4). As above any transformation that would require picking a value for the Hubble constant or a cosmological model was avoided. The same distance scaling factor used for the SDSS and MS data, as described in Section 5.5, Item 7, namely  $d_{uniform} = 3.2 \times 10^{-3}$ , was used to derive the same Voronoi quantities found for the SDSS in Section 5.5.

As in the previous two cases, in order to mimic the BB and SOM class methods a filter was applied to the AKM densities to produce the 10 uniform classes found in Table 3 of Paper I:

$$AKM_{class} = 11 - \text{round}(((\log_{10}(AKM_{density})/5.6947) \times 40) - 13) \quad (7)$$

---

<sup>16</sup>See Cheng (2005); Peacock (1999); Hogg (1999) for more on the luminosity distance.

<sup>17</sup>The final number of points described in Paper I is incorrect. The 144,700 quoted was before the removal of the 55'' and boundary value points, not after.

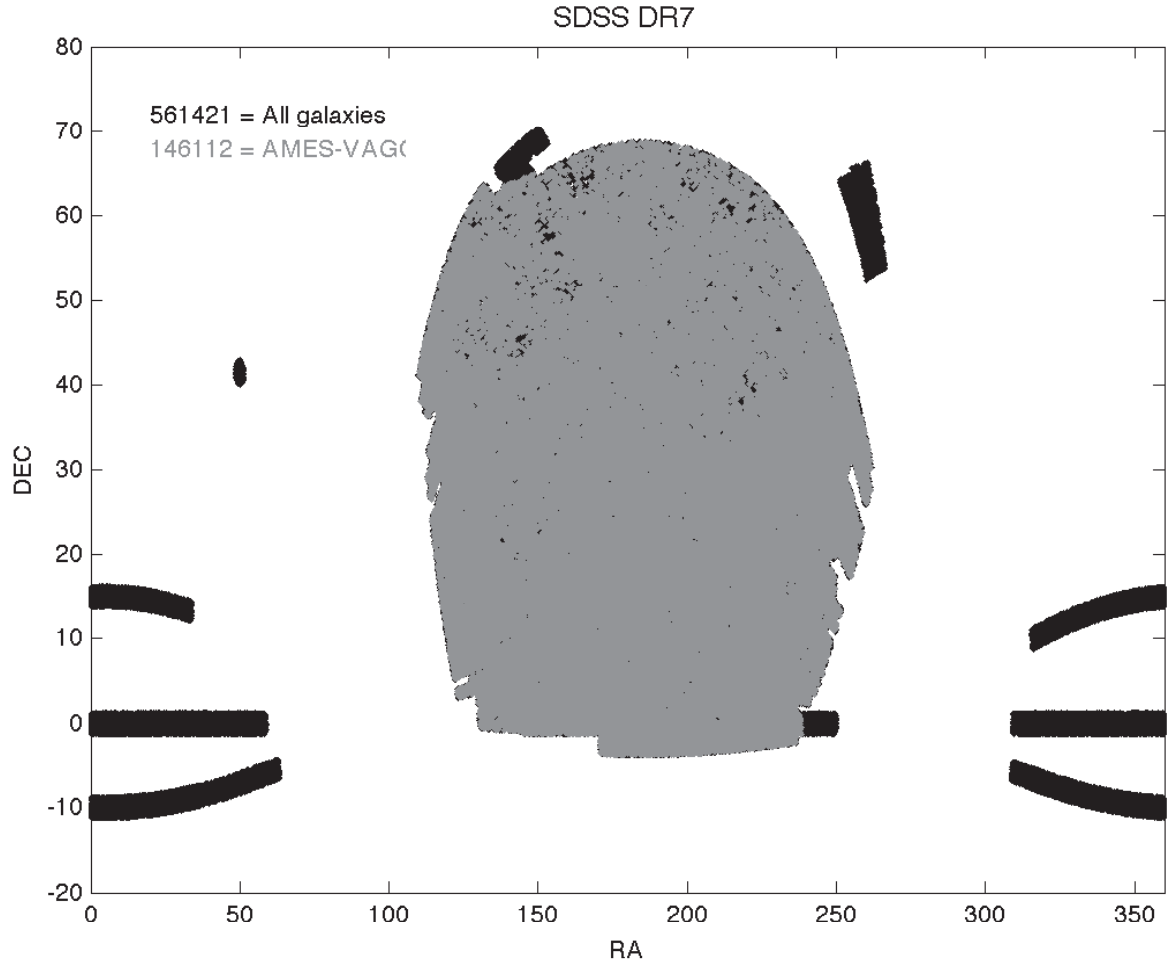


Fig. 9.— Plot of the entire SDSS DR7 Main-Like Galaxy Sample from the NYU-VAGC catalog (both black and gray points). The points in gray are those of the volume limited sub-sample derived from stage two of the catalog as described in Section 5.1. The black points were eliminated from the volume limited sample as a result of redshift and absolute luminosity cuts, ( $z < 0.12$  and  $M_R^{0.1} < -20.0751$ ), and the desire for a contiguous geometric sample.

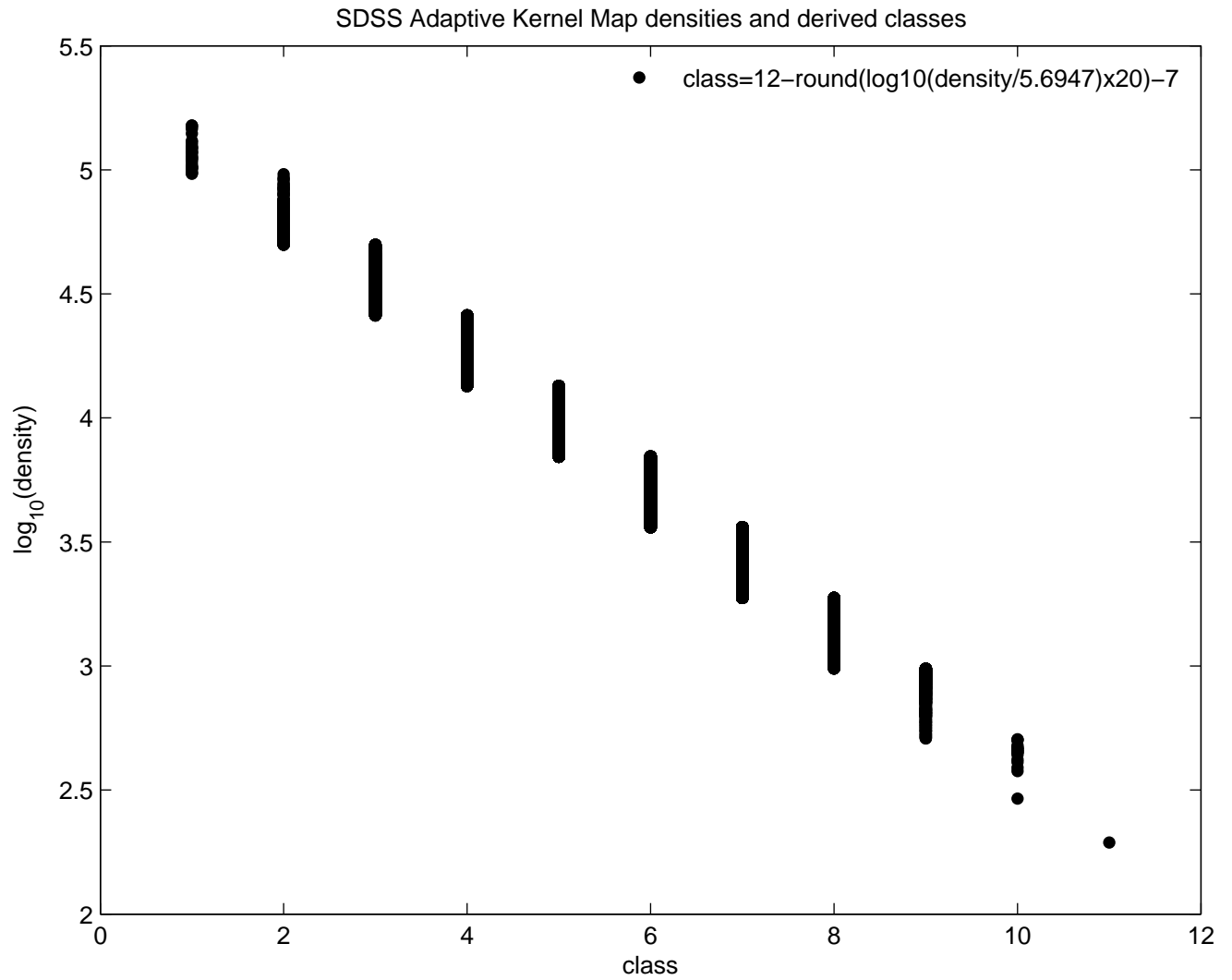


Fig. 10.— Plot of Adaptive Kernel Map densities versus their derived classes using Eq. 5 in the text and figure legend.

### 5.11. Structure Catalog Information: Electronic-Only Files

For each of the 3 data sets we have constructed a flat ASCII file, the columns of which contain information, one row for each galaxy, of use for assembling many kinds of structure catalogs of interest. Many of the entries echo data from the NYU-VAGC data archive, for the reader’s convenience in constructing and exploring structure catalogs derived from the new results. The names of these electronically accessible files are `sdss_master.txt`, `ms_master.txt` and `poissmaster.txt`, and the rest of this sections describes their contents and a provides a few notes on there use in constructing structure catalogs. The terms “Max-structure” and “Min-structure” mean HOP groups associated with local maxima and local minima, respectively.

Table 4:: Column Identifiers: 146,112 SDSS Galaxies

Column Number	Variable Name	Description
1	objid(high) <sup>a</sup>	NYU-VAGC Identifier
2	objid(low) <sup>a</sup>	NYU-VAGC Identifier
3	id2	running index
4	vagc_specobjid	NYU-VAGC Spectrum ID
5	x	x-Coordinate
6	y	y-Coordinate
7	z	z-Coordinate
8	ra	right ascension
9	dec	declination
10	redshift	observed redshift
11	redshift_err	redshift error
12	u	apparent u magnitude
13	g	apparent g magnitude
14	r	apparent r magnitude
15	i	apparent i magnitude
16	z	apparent z magnitude
17	U	absolute u magnitude
18	G	absolute g magnitude
19	R	absolute r magnitude
20	I	absolute i magnitude
21	Z	absolute z magnitude
22	J	absolute j magnitude
23	H	absolute h magnitude
24	K	absolute k magnitude
25	p50_u	Petrosian 50% u radius
26	p50_g	Petrosian 50% g radius

Continued on next page

Table 4 – continued from previous page

Column Number	Name	Description
27	p50_r	Petrosian 50% r radius
28	p50_i	Petrosian 50% i radius
29	p50_z	Petrosian 50% z radius
30	p90_u	Petrosian 90% u radius
31	p90_g	Petrosian 90% g radius
32	p90_r	Petrosian 90% r radius
33	p90_i	Petrosian 90% i radius
34	p90_z	Petrosian 90% z radius
35	dCM/R_Voronoi	centroid $\rightarrow$ point (normalized)
36	R_Voronoi/dUniform <sup>b</sup>	cell volume / total volume
37	R_Max	Distance from sample to farthest vertex
38	R_Min	Distance from sample to nearest vertex
39	R_Max / R_Min	Elongation
40	cnWinners	Class ID with most votes
41	volume	Cell volume
42	bb_vol_lev	Level ID BB(vol) <sup>c</sup>
43	bb_vol_blk	Block ID BB(vol) <sup>c</sup>
44	bb_den_lev	Level ID BB(den) <sup>d</sup>
45	bb_den_blk	Block ID BB(den) <sup>d</sup>
46	f55	0; but 1 if cell collision test fails
47	fbad	0; but 1 if boundary test fails
48	density_akm	KDE density
49	bandwidth_akm	KDE bandwidth
50	levels_akm	KDE density level
51	ID(Vor,+) )	Max-structure ID; HOP $f = 1/\text{volume}$
52	ID(Vor,-)	Min-structure ID; HOP $f = 1/\text{volume}$
53	ID(AKM,+)	Max-structure ID; HOP $f = 1/\text{density\_akm}$
54	ID(AKM,-)	Min-structure ID; HOP $f = 1/\text{density\_akm}$
55	ID(SOM,+)	Max-structure ID; HOP $f = \text{cnWinners}$
56	ID(SOM,-)	Min-structure ID; HOP $f = \text{cnWinners}$
57	ID(BB(volume),+)	Max-structure ID; HOP $f = n(\text{blk})/\text{volume}$ ; BB(vol) <sup>b</sup>
58	ID(BB(volume),-)	Min-structure ID; HOP $f = n(\text{blk})/\text{volume}$ ; BB(vol) <sup>b</sup>
59	ID(BB(density),+)	Max-structure ID; HOP $f = n(\text{blk})/\text{volume}$ ; BB(den) <sup>c</sup>
60	ID(BB(density),-)	Min-structure ID; HOP $f = n(\text{blk})/\text{volume}$ ; BB(den) <sup>c</sup>

(a) These long integer identifiers are divided into two parts; the most significant 9 digits (high) and least significant (low). Using Matlab, after executing load `sdss_master.txt` the string `[ int2str( sdss_master( :, 1 ) ) int2str( sdss_master( :, 2 ) ) ]` rejoins the two parts.



- (b) dUniform, the average distance between objects in the sample, equals 3.2e-3 redshift units.
- (c) Bayesian Block analysis based on Voronoi cell volume.
- (d) Bayesian Block analysis based on Voronoi cell density.

The last 10 columns of structure IDs can be used to construct catalogs as follows. Let the MatLab variable `index_structures` denote an array containing the integers in one of these columns, This contains, for each galaxy G, the index of the structure to which the galaxy is assigned by the converged HOP iteration. Then one can construct an array containing these structure IDs using the MatLab command

```
ids = unique( index_structures )
```

which is also just the array 1, 2, ..., M where M is the number of structures HOP has identified. Then for any structure ID m satisfying  $1 \leq m \leq M$  the indices of the galaxies in that structure (indexed in the original raw data array, including galaxies that later failed the f55/fbad tests) can be found from

```
galaxy_indices = find( index_structures == ids(m) );
```

This allows one to compute many things for that structure, such as the xyz-coordinates of all the galaxies in it, the volume of the structure (as the sum of the Voronoi volumes), the number of galaxies in it, and the density in galaxies per unit volume – using the corresponding data in the other columns of the master file.

The following two tables give similar identifications for the MS and Poisson data files. Fewer entries have been defined for these data sets, but the meanings of the parameters which are in common are the same.

Table 5:: **Column Identifiers: 171,388 MS Galaxies**

Column Number	Variable Name	Description
1	objid	NYU-VAGC Identifier
2	id2	running index
3	x	x-Coordinate
4	y	y-Coordinate
5	z	z-Coordinate
6	ra	right ascension
7	dec	declination
8	redshift	observed redshift

Continued on next page

Table 5 – continued from previous page

Column Number	Name	Description
9	u	apparent u magnitude
10	g	apparent g magnitude
11	r	apparent r magnitude
12	i	apparent i magnitude
13	z	apparent z magnitude
14	U	absolute u magnitude
15	G	absolute g magnitude
16	R	absolute r magnitude
17	I	absolute i magnitude
18	Z	absolute z magnitude
19	dCM/R_Voronoi	centroid $\rightarrow$ point (normalized)
20	R_Voronoi/dUniform <sup>a</sup>	cell volume / total volume
21	R_Max	Distance from sample to farthest vertex
22	R_Min	Distance from sample to nearest vertex
23	R_Max / R_Min	Elongation
24	cnWinners	Class ID with most votes
25	volume	Cell volume
26	bb_vol_lev	Level ID BB(vol) <sup>b</sup>
27	bb_vol_blk	Block ID BB(vol) <sup>b</sup>
28	bb_den_lev	Level ID BB(den) <sup>c</sup>
29	bb_den_blk	Block ID BB(den) <sup>c</sup>
30	f55	0; but 1 if cell collision test fails
31	fbad	0; but 1 if boundary test fails
32	density_akm	KDE density
33	bandwidth_akm	KDE bandwidth
34	levels_akm	KDE density level
35	ID(Vor,+)	Max-structure ID; HOP $f = 1/\text{volume}$
36	ID(Vor,-)	Min-structure ID; HOP $f = 1/\text{volume}$
37	ID(AKM,+)	Max-structure ID; HOP $f = 1/\text{density\_akm}$
38	ID(AKM,-)	Min-structure ID; HOP $f = 1/\text{density\_akm}$
39	ID(SOM,+)	Max-structure ID; HOP $f = \text{cnWinners}$
40	ID(SOM,-)	Min-structure ID; HOP $f = \text{cnWinners}$
41	ID(BB(volume),+)	Max-structure ID; HOP $f = n(\text{blk})/\text{volume}$ ; BB(vol) <sup>b</sup>
42	ID(BB(volume),-)	Min-structure ID; HOP $f = n(\text{blk})/\text{volume}$ ; BB(vol) <sup>b</sup>
43	ID(BB(density),+)	Max-structure ID; HOP $f = n(\text{blk})/\text{volume}$ ; BB(den) <sup>c</sup>
44	ID(BB(density),-)	Min-structure ID; HOP $f = n(\text{blk})/\text{volume}$ ; BB(den) <sup>c</sup>

(a) dUniform, the average distance between objects in the sample, equals 3.2e-3 redshift units.

(b) Bayesian Block analysis based on Voronoi cell volume.

(c) Bayesian Block analysis based on Voronoi cell density.

Table 6:: **Column Identifiers: 144,700 Random Points**

Column Number	Variable Name	Description
1	id2	running index
2	x	x-Coordinate
3	y	y-Coordinate
4	z	z-Coordinate
5	ra	right ascension
6	dec	declination
7	redshift	observed redshift
8	dCM/R_Voronoi	centroid $\rightarrow$ point (normalized)
9	R_Voronoi/dUniform <sup>a</sup>	cell volume / total volume
10	R_Max	Distance from sample to farthest vertex
11	R_Min	Distance from sample to nearest vertex
12	R_Max / R_Min	Elongation
13	cnWinners	Class ID with most votes
14	volume	Cell volume
15	bb_vol_lev	Level ID BB(vol) <sup>b</sup>
16	bb_vol_blk	Block ID BB(vol) <sup>b</sup>
17	bb_den_lev	Level ID BB(den) <sup>c</sup>
18	bb_den_blk	Block ID BB(den) <sup>c</sup>
19	f55	0; but 1 if cell collision test fails
20	fbad	0; but 1 if boundary test fails
21	density_akm	KDE density
22	bandwidth_akm	KDE bandwidth
23	levels_akm	KDE density level
24	ID(Vor,+)	Max-structure ID; HOP $f = 1/\text{volume}$
25	ID(Vor,-)	Min-structure ID; HOP $f = 1/\text{volume}$
26	ID(AKM,+)	Max-structure ID; HOP $f = 1/\text{density\_akm}$
27	ID(AKM,-)	Min-structure ID; HOP $f = 1/\text{density\_akm}$
28	ID(SOM,+)	Max-structure ID; HOP $f = \text{cnWinners}$
29	ID(SOM,-)	Min-structure ID; HOP $f = \text{cnWinners}$
30	ID(BB(volume),+)	Max-structure ID; HOP $f = n(\text{blk})/\text{volume}$ ; BB(vol) <sup>b</sup>
31	ID(BB(volume),-)	Min-structure ID; HOP $f = n(\text{blk})/\text{volume}$ ; BB(vol) <sup>b</sup>
32	ID(BB(density),+)	Max-structure ID; HOP $f = n(\text{blk})/\text{volume}$ ; BB(den) <sup>c</sup>
33	ID(BB(density),-)	Min-structure ID; HOP $f = n(\text{blk})/\text{volume}$ ; BB(den) <sup>c</sup>

- (a) dUniform, the average distance between objects in the sample, equals 3.2e-3 redshift units.
- (b) Bayesian Block analysis based on Voronoi cell volume.
- (c) Bayesian Block analysis based on Voronoi cell density.

### 5.12. Void Catalog Information: Electronic-Only Files

For each of the 3 data sets we have also constructed a flat ASCII file containing identities and descriptions of the HOP voids. The names of these electronically accessible files for the SDSS, MS and Poisson data are `delaunay_voids_sdss.txt`, `delaunay_voids_ms.txt` and `delaunay_voids_poiss.txt`, respectively. All three files have the format given in Table 7. The identification number is a running index for the 458,173, 503,832, and 465,357 voids in the three cases, respectively. The next two columns contain the number of tetrahedra and galaxies in the void, followed by the void effective radius in Eq. (1), convexity (see the caption to Fig. 7), and distance from the augmented hull of the full data set. The columns beginning with number seven give the identities of the galaxies circumscribing the void; these are the running index values *id2* in Tables 4, 5, and 6, respectively. These rows contain a variable number of galaxy IDs. All rows with less than the maximum number (25, 29, and 23 in the three cases, respectively) of galaxy IDs are padded with zeros to yield fixed record-length files. These lengths are 31, 35 and 29 in the three cases, respectively.

Table 7: Delaunay Voids

Column Number	Variable Name	Description
1	VID	Void identification number
2	$N_{\text{tet}}$	Number of tetrahedra
3	$N_{\text{gal}}$	Number of galaxies
4	$R_{\text{eff}}$	Effective radius (Mpc)
5	<i>cvx</i>	Convexity
6	<code>dist_min</code>	Distance from hull
7 ...	<code>gid</code>	Galaxy IDs

## 6. Appendix B: Zwicky Morphological Analysis of Topological Noise Effects

The effect of sampling or measurement imperfections on data used to estimate a distribution, especially in higher dimensions, is always much more complicated than, say, for the case of simple parameter estimation. In the current spatial statistics context, the various processes discussed in Section 3.3 (and here, in the abuse of terminology described in that section, termed *noise*) can have several effects on the estimated structures. Table 8 is a *morphological box*, a device pioneered

by Zwicky (1948, 1957) to facilitate complete investigation of parameter spaces. The first column (a) of this chart lists all six possible effects noise of any kind may have on a specific structure, including creation of a new structure and modification or destruction of an existing one. Column (b) gives the accompanying net change in the number of structures. Given the “before” size of a structure shown in the headings columns (c) - (f) the “after” size (with noise) is entered in the rows below. The whole point of this construct is to bring to light effects that might not be obvious at first thought. For example, noise may actually bring about the apparent merger of two structures into one (row E), e.g. turning two small structures into one medium structure as in box E(d). A conclusion derivable from this matrix is that the common procedure of eliminating the smallest structures in the size distribution may be only partially effective at de-noising.

Table 8: **Zwicky Morphological Matrix:** Effect of Noise on Numbers and Sizes of Structures

	(a) <b>Noise Effect</b>	(b) $\delta N$	(c) <b>Nonexistent</b>	(d) <b>Small</b>	(e) <b>Medium</b>	(f) <b>Large</b>
A	Create	+1	Small	—	—	—
B	Separate into Two	+1	—	Small-	Small	Medium
C	Reduce content	0	—	Small-	Small	Medium
D	Increase content	0	—	Medium	Large	Large+
E	Merge	-1	—	Medium	Large	Large+
F	Destroy	-1	—	Null	Null	Null

---

Note: The size indicators here are only rough and nominal. The plus and minus signs are to be interpreted as “even larger” or “even smaller,” respectively.

## REFERENCES

- Abazajian, K.N. et al. 2009, ApJS, 182, 543
- Ahn, C., et al. 2012, arXiv:1307.7735 (Submitted to ApJS)
- Aikio, J., & Mahonen, P., 1998, ApJ, 497, 534.
- Amendola, L., Frieman, J., & Waga, I. 1999, MNRAS, 309, 465
- Angulo, R., Chen, R., Hilbert, S., & Abel, T. 2013, submitted to MNRAS, arXiv:1309.1161v2
- Aragon-Calvo, M., Jones, B., van de Weygaert, R., & van der Hulst, J., 2007, A&A, 474, 315.
- Aragon-Calvo, M., Platen, E., van de Weygaert, R. & Szalay, A. 2010a, ApJ, 723, 364.
- Aragon-Calvo, M. A., van de Weygaerti, R., Araya-Melo, P. A., Platen, E., & Szalay A. S. 2010b, MNRAS, 404, L89.
- Aragon-Calvo, M. A., & Szalay A. S. 2013, MNRAS, 428, 3409.
- Aubert, D., Pichon. C and Colombi, S. 2004, MNRAS, 352, 376
- Beygu, B., Kreckel, K., van de Weygaert, R., van der Hulst, J. M., van Gorkom, J. H. 2013, AJ, 145, 120
- Blanton, M. R. et al. 2005, AJ, 129, 2562
- Bolejko, Krzysztof, Clarkson, Chris, Maartens, Roy, Bacon, David, Meures, Nikolai, Beynon, E. 2012, Phys. Rev. Lett., 110, 021302
- Bos, E., van de Weygaert, R., Dolag, K., & Pettorino, V.(2012) MNRAS, 426, 440
- Carlsson, G, 2013 [math.stanford.edu/~gunnar/actanumericathree.pdf](http://math.stanford.edu/~gunnar/actanumericathree.pdf)
- Cautun, M. & van de Weygaert, R. 2011, The DTFE public software: The Delaunay Tessellation Field Estimator code, 2011 <http://asterisk.apod.com/viewtopic.php?f=35&t=23588>
- Chen, Y-C., Genovese, C., & Wasserman, L. 2013, “Uncertainty Measures and Limiting Distributions for Filament Estimation,” arXiv:1312.2098v1
- Ceccarelli, L., Paz, D., Lares, M., Padilla, N., & Garcia Lambas, D. 2013, “Clues on void evolution I: Large scale galaxy distributions around voids,” arXiv:1306.5798v1
- Chazal, F., Fasy, B., Lecci, F., Rinaldo, A., Singh, A. & Wasserman, L. 2014, “On the Bootstrap for Persistence Diagrams and Landscapes,” arXiv:1311.0376v2
- Cheng, T.P. 2005 “Relativity, gravitation, and cosmology: a basic introduction”, ISBN 9780198529576, Pub. Oxford University Press

- Chincarini, G. & Rood, H.J. 1976, ApJ, 206, 30
- Cisewski, J., Croft, R., Freeman, P., Genovese, R., Khandai, N., Ozbek, M., & Wasserman, L. 2014, “Nonparametric 3D map of the IGM using the Lyman-alpha forest,” arXiv:1401.1867v1
- Coil, A. 2012, “Large Scale Structure of the Universe,” Volume 8., Section 9, in Planets, Stars and Stellar Systems Oswalt, T. D., ed. Springer: New York. <http://ned.ipac.caltech.edu/level5/March12/Coil/Coil9.html>
- Colberg, J., Pearce, F. et al. 2008 MNRAS, 387, 933.
- Colless, M.M. et al. 2001, MNRAS, 328, 1039
- Choi Y. et al. 2010 ApJS, 109, 181
- Croton D.J. et al., 2005, MNRAS, 356, 1155
- Daley, D. & Vere-Jones, D., 2003, An Introduction to the Theory of Point Processes: Vol. I: Elementary Theory and Methods, 2nd Edition, Springer-Verlag: New York
- DAbrusco, R., Fabbiano, G., Djorgovski, G., Donalek, C., Laurino, O. and G. Longo, G. 2012, ApJ, 755, 92
- D’Aloisio, A. & Furlanetto, S. (2007), MNRAS, 382, 860
- de Berg, M., Cheong, O., van Kreveld, M., Overmars, M. 1997, Computational Geometry: Algorithms and Applications, Springer-Verlag: New York
- Edelsbrunner, H. 1987, Algorithms in Combinatorial Geometry, EATCS Monographs on Theoretical Computer Science, Vo. 10, Springer-Verlag, New York
- Edelsbrunner, H., Letscher, D., & Zomorodian, A., 2002 Discrete Computational Geometry, 28, 511
- Edelsbrunner, H. & Harer, J., 2010, Computational Topology, American Mathematical Society: Providence, RI.
- Einasto, J., Einasto, M., & Gramann, M.(1989) MNRAS, 238, 155
- Einasto, M., Liivamägi, L., Tempel, E., Saar, E., Tago, E., Einasto, P., I. Enkvist, I., Einasto, J., Martinez, V., Heinämäki, P., & Nurmi, P.(2011), ApJ, 736, 51
- Einasto, M., Liivamägi, L. J., Tempel, E., Saar, E., Vennik, J., Nurmi, P., Gramann, M., Einasto, J., Tago, E., Heinmki, P., Ahvensalmi, A., & Martnez, V.(2012) A&A, 542, 36
- Einasto, J., Suhhonenko, I., Htsi, G., Saar, E., Einasto, M., Liivamägi, L. J., Müller, V., Starobinsky, A. A., Tago, E., Tempel, E. 2011, A&A534, 128

- Einasto, M., Lietzen, H., Tempel, E., Gramann, M., Liivamägi, & Einasto, J., 2014, *A&A*562, A87
- Einasto, J. 2014, “Dark Matter and Cosmic Web Story”, Edited by Jaan Einasto. Published by World Scientific Publishing Co. Pte. Ltd., 2013. ISBN 9789814551052
- Eisenstein, D. & Hut, P. 1998, *ApJ*, 498, 137
- Elyiv, A., Karachentsev, I., Karachentseva, V., Melnyk, O., & Makarov, D.(2013) *Astrophysical Bulletin* 68, 1-12, arXiv:1302.2369v2
- El-Ad, H., Piran, T. & da Costa, L.(1996) *ApJ*, L13
- El-Ad, H., (1997) “The (> Half) Empty Universe, in From Quantum Fluctuations to Cosmological Structures, ASP Conference Series, 126, 313.
- El-Ad, H., & Piran, T. (1997) *ApJ*, 491, 421
- El-Ad, H., & Piran, T. (2000) *MNRAS*, 313, 553
- El-Ad, H., Piran, T. & da Costa, L. 1997, *MNRAS*, 287, 790
- Falck, B., Neyrinck, M. & Szalay, A. 2012, Talk summary to appear in the Proceedings of the 13th Marcel Grossmann Meeting (MG13), Stockholm, July 2012, arXiv:1309.4787N
- Fasy, B., Lecci, F., Rinaldo, A., Wasserman, L., & Singh, A. 2014, “Statistical Inference for Persistent Homology: Confidence Sets for Persistence Diagrams,” arXiv:13037117v2
- Forman, R. 2002, *Séminaire Lotharingien de Combinatoire* 48, B48c
- Gaite, J., 2009, *Journal of Cosmology and Astroparticle Physics*, 1, 11
- Gazis, P. R., Levit, C. & Way, M. J. 2010, *PASP*, 122, 1518
- Gerber, S., Bremer, P. , Pascucci, V. , & Whitaker, R., 2010, *IEEE Transactions on Visualization and Computer Graphics*, 16, 1271
- Gladders, M. & Yee, H. 2000, *AJ*, 120, 2148
- Gott, J., Hambrick, D. et al. 2008, *ApJ*, 675, 16
- Gregory, S. & Thompson, L. 1978, *ApJ*, 222, 784
- Gyulassy, A. & Natarajan, V.(2005), Topology-based simplification for feature extraction from 3D scalar fields, *Visualization*, 2005. VIS 05. IEEE
- Hahn, O., Porciani, C., Carollo, C., Marcella, C., & Dekel, A. 2007, *MNRAS*, 375, 489
- Hahn, O., Carollo, C., Marcella, C., Porciani, C., & Dekel, A. 2007, *MNRAS*, 381, 41



- Hamaus, N., Wandelt, B., Sutter, P., Lavaux, G. & Warren, M. arXiv:1307.2571v1
- Hamaus, N., Sutter, P., & Wandelt, B., 2014, arXiv:1403.5499
- Hidding, J., Shandarin, S., & van de Weygaert, R. 2014, MNRAS, 437, 3442
- Higuchi, Y., Oguri, M., & Hamana, T., 2011, MNRAS, 432, 1021, arXiv:1211.5966v2
- Hogg, D.W. 1999, arXiv:astro-ph/9905116v4
- Holmberg, E. 1969, Arkiv För Astronomi, 5, 305
- Hoyle, F. & Vogeley, M. 2002, ApJ, 566, 641
- Ivezić, Z., Connolly, A., VabderPlas, J., & Gray, A., Statistics, Data Mining, and Machine Learning in Astronomy, 2014, Princeton University Press.
- Jackson, B., Scargle J., Cusanza, C., Barnes, D., Kanygin, R., Sarmiento, R., Subramaniam, S., Tzu-Wang, C. 2010, Optimal Partitions of Data In Higher Dimensions, in Proceedings of the 2010 Conference on Intelligent Data Understanding, eds: Ashok N. Srivastava, Nitesh Chawla, Philip Yu and Paul Melby, NASA Ames Research Center: Mountain View
- James, J.B. et al. 2009, MNRAS, 394, 454
- Jasche, J. et al. 2010, MNRAS, 406, 60
- Jennings, E., Li, Y., & Hu, W.(2013) “The abundance of voids and the excursion set formalism,” arXiv1304.6087
- Joeveer, M., Einasto, J. & Tago, M. 1977, Tartu Astrofüüs. Obs. Preprint, Nr. A-1, 45
- Joeveer, M., Einasto, J. & Tago, M. 1978, MNRAS, 185, 357
- Joeveer, M. & Einasto, J. 1978, in The large scale structure of the universe; Proceedings of the Symposium, Tallin, Estonian SSR, September 12-16, 1977. (A79-13511 03-90) Dordrecht, D. Reidel Publishing Co., 1978, p. 241-250
- Kauffmann, G. & Fairall, A. 1991, MNRAS, 1991, 248, 313
- Knebe, A., Knollmann, et al. 2011, MNRAS, 415, 2293
- Knebe, A., Pearce, F. et al. 2013, MNRAS, 435, 1618
- Koenderink, J. 1990, Soliud Shape, MIT Press, Cambridge, Mass.
- Kopylov, A. & Kopylova, F. 2002, Astron. Astrophys. 382, 389. Data at: <http://vizier.cfa.harvard.edu/viz-bin/VizieR?-source=J/A+A/382/389>
- Krause, E., Chang, T.-C., Dor, O., & Umetsu, K. 2013, ApJ, 762, 20

- Lavaux . G. & Wandelt, B. (2010) MNRAS, 403, 1392
- Lavaux . G. & Wandelt, B. (2012) ApJ, 754, 109
- Flaglets for studying the large-scale structure of the Universe, Leistedt, B., Peiris, H., & McEwen, J. 2013, Proceedings of Wavelets and Sparsity XV, SPIE Optics and Photonics, arXiv:1308.5480
- Lavaux, G. & Wandelt, B. (2012) ApJ, 754, 109
- Liivamägi, L., Tempel, E., & Saar, E. 2012, A&A539, A80
- Longair, M.S. 1978, “Personal View - The Large Scale Structure of the Universe,” in The large scale structure of the universe; Eds. M. Longair and J. Einasto, Proceedings of the Symposium, Tallin, Estonian SSR, September 12-16, 1977. (A79-13511 03-90) Dordrecht, D. Reidel Publishing Co., 1978,
- Longair, M.S. & Einasto, J. 1978, “The Large scale structure of the universe”: Symposium no. 79 held in Tallinn, Estonia, U.S.S.R., September 12-16, 1977, Dordrecht, Holland ; Boston : D. Reidel Pub. Co., 1978.
- Lowen, S. & Teich, M. 2005, Fractal-Based Point Processes, John Wiley & Sons: Hoboken, New Jersey
- Martinez, V. & Saar, E. 2002, Statistics of the Galaxy Distribution, Chapman & Hall/CRC, Boca Raton
- Marzban, C., Yurtsever, U. 2011, Baby morse theory in data analysis, in Proceedings of the 2011 workshop on Knowledge discovery, modeling and simulation, ACM New York, NY
- Milnor, J., 1969, Morse Theory, Annals of Mathematics Studies, Princeton University Press.
- Müller, V., Hoffman, K. & Nuza, S.E. 2011, Baltic Astronomy, 20, 259
- McBride, C.K. et al. 2011, ApJ, 739, 85
- Melchior, P., Sutter, P., Sheldon, E., Krause, E. & Wandelt, B. arXiv:1309.2045v1, submitted to MNRAS
- Neyrinck, M.C., Gnedin, N. & Hamilton, J. 2005, MNRAS, 356, 1222
- Neyrinck, M.C., 2008, MNRAS, 386, 2101
- Neyrinck, M.C., Szapudi, I. & Szalay, A.S. 2009, ApJ, 698, 90
- Neyrinck, M.C., Aragon-Calvo, M., Jeong, D., & Wang, X. 2013, arXiv:1309.6641
- Nadathur, S. & Hotchkiss, S. 2014, MNRAS, 440, 1248

- Okabe, A., Boots, B., Sugihara, K., & Chiu, S. N. 2000, *Spatial Tessellations: Concepts and Applications of Voronoi Diagrams*, John Wiley and Sons, Ltd., New York, Second Edition
- Muñoz-Cuartas, J.C. & Müller, V. 2012, *MNRAS*, 423, 1583
- Pan, D., Vogeley, M., Hoyle, F., Choi, Y.-Y., Park, C. 2012, *MNRAS*, 421, 926
- Pandey, B., White, S., Springel, V. & Angulo, R. 2013, *MNRAS*, 435, 2968, arXiv:1301.3789v2
- Paranjape, A., Lam, T., & Sheth, R. 2011, *MNRAS*, 420, 1648
- Park, C., Choi, Y., Kim, J., Gott, J., Kim, S., Kim, K. 2012, *ApJ*, 759, 7
- Park, C., Pranav, P., Chingangbam, P., van de Weygaert, R., Jones, B., Vegter, G., Kim, I., Hidding, J., & Hellwing, W. 2013, *JKAS*, 46, 125 arXiv:1307.2384
- Patiri, S., Prada, F., Holtzman, J., Klypin, A. & Betancort-Rijo, J. 2006, *MNRAS*, 372, 1710
- Peacock, J.A. 1999, “Cosmological physics”, ISBN 9780521422703, Pub. Cambridge University Press
- Peebles, J. 2001, *Ap&SS*, 31,403
- Peebles, J. 1980, *The large-scale structure of the universe*, Princeton University Press: Princeton
- Peebles, J. 1984, *Hierarchical Clustering*, in *Clusters and Groups of Galaxies*, Astrophysics and Space Science Library Volume, 111, 405
- Peebles, J. 2001, *ApJ*, 557, 495
- Platen, E., van de Weygaert, R., & Jones, B. 2007, *MNRAS*, 380, 551
- Platen, E., van de Weygaert, R., Jones, B. Vegter, G., & Aragon Calvo, M. 2011, *MNRAS*, 416, 2494
- Perparata, F. & Shamos, M. 1985, *Computational Geometry: an Introduction*, Springer-Verlag, New York
- Ricciardelli, E., Quilis, J. and Varela, J 2014, *MNRAS*, 440, 601, arXiv:1402.2976
- Rojas, R., Vogeley, M., Hoyle, F. & Brinkman, J 2004, *ApJ*, 617, 50
- Rozo, E., Rykoff, E., Bartlett, J., & Melin, J. 2014, *redMaPPer III: A detailed comparison of the Planck 2013 and SDSS DR8 RedMaPPer Cluster Catalogs*, arXiv:1401.7716
- Rozo, E., Rykoff, E., 2013, *redMaPPer II: X-ray and SZ Performance Benchmarks for the SDSS Catalog*, arXiv:1303.3373
- Rykoff, E., Rozo, E., Busha, M., Cunha, C., Finoguenov, A., Evrard, A., Hao, J., Koester, B. P.; Leauthaud, A.; Nord, B., Pierre, M., Sadibekova, T., Sheldon, E., & Wechsler, R., 2013, *redMaPPer I: Algorithm and SDSS DR8 Catalog*, arXiv:1303.3562

- Scargle, J., Norris, J., Jackson, B., and Chiang, J. 2013, ApJ, 764, 167
- Schaap, W. 2007, DFTE: the Delaunay Tessellation Field Estimator, Thesis:  
<http://dissertations.ub.rug.nl/faculties/science/2007/w.e.schaap/>
- Schmidt, J., Ryden, B., & Melott, A.(2001) ApJ, 546, 609
- Schwarzschild, B. M., 1982, Physics Today, 35, 17
- Shandarin, S.F., Sheth, J.V. & Sahni, V. 2004, MNRAS, 353, 162
- Shectman, S.A. et al. 1996, ApJ, 470, 172
- Skory, S., Turk, M., Norman, M., & Coil, L. 2010, ApJS, 191, 43
- Skrutskie, M.F. et al. 2005, AJ, 131, 1163
- Snyder, D. & Miller, M. 1991, Random Point Processes in Time and Space, Springer-Verlag: New York.
- Sousbie, T. 2013, DisPerSE: robust structure identification in 2D and 3D, arXiv1302.6221S, cf. <http://asterisk.apod.com/viewtopic.php?f=35&t=30806> with software at <http://www2.iap.fr/users/sousbie/web/html/indexd41d.html?>
- Sousbie, T. 2011, MNRAS, 414, 350
- Sousbie, T., Pichon, C. & Kawahara, H. 2011, MNRAS, 414, 384
- Springel, V. 1999, PhD. Thesis: On the Formation and Evolution of Galaxies, <http://www.mpa-garching.mpg.de/~volker/>
- Springel, V., et al. 2005, Nature, 435, 629
- Strauss, M. A., et al. 2002 AJ, 124, 1810
- Sutter, P., Lavaux, G., Wandelt, B. & Weinberg, D.(2012) ApJ, 761, 44
- Tavasoli, S., Vasei, K. & Mohayaee, R. 2013, A&A553, A15.
- Tegmark, M., Eisenstein, D., et al., 2006 Physical Review D, 74, 123507
- Tempel, E., Tamm, A., Gramann, M., Tuvikene, T., Liivamäggi, L., Suhhonenko, I., Kipper, R., Einasto, M., & Saar, E. 2014, arXiv:1402.1350v1
- Thompson, L.A. & Gregory, S.A. 2011 arXiv:1109.1268
- Tift, W.G. & Gregory, S.A. 1978 “Observations of the Large Scale Distribution of Galaxies” in The large scale structure of the universe; Eds. M. Longair and J. Einasto, Proceedings of the Symposium, Tallin, Estonian SSR, September 12-16, 1977. (A79-13511 03-90) Dordrecht, D. Reidel Publishing Co., 1978, p. 267

- Tully, R. & Fisher, J. 1978 “Nearby Small Groups of Galaxies,” in The large scale structure of the universe; Eds. M. Longair and J. Einasto, Proceedings of the Symposium, Tallin, Estonian SSR, September 12-16, 1977. (A79-13511 03-90) Dordrecht, D. Reidel Publishing Co., 1978, p.31
- Turk, M, Smith, B. D., Oshi, J., Kkory, S., Skillman, S., Abel, T., & Norman, M. ApJS, 192, 9
- Valageas, P. & Clerc, N. 2012, arXiv:1205.4847
- van de Weygaert, R., Jones, B., Platen, E., & Aragon-Calvo, M. 2009, in Sixth International Symposium on Voronoi Diagrams, 2009, 3, arXiv:0912.3448
- van de Weygaert, R., Vegter, G., Platen, E., Eldering, B., & Kruithof, N. 2010, in Seventh International Symposium on Voronoi Diagrams, 2010, 3, arXiv:0912.3448 arXiv:1006.2765
- van de Weygaert, R., Kreckel, K., Platen, E., Beygu, B., van Gorkom, J. H., van der Hulst, J. M., Aragn-Calvo, M. A., Peebles, P. J. E., Jarrett, T., Rhee, G., Kovač, K., Yip, C.-W. 2011, The Void Galaxy Survey, in Environment and the Formation of Galaxies: 30 years later, Astrophysics and Space Science Proceedings, ISBN 978-3-642-20284-1. Springer-Verlag Berlin Heidelberg, 2011, p. 17
- van de Weygaert, R., Pranav, P., Jones, B., Bos, P., Vegter, G., Edelsbrunner, H., Teillaud, M., Hellwing, W., Park, C., Hidding, J., and Wintraecken, M. 2011, Probing dark energy with alpha shapes and betti numbers, arXiv:1110.5528
- van de Weygaert, R.; Vegter, G.; Edelsbrunner, H.; Jones, B.; Pranav, P.; Park, C.; Hellwing, W.; Eldering, B.; Kruithof, N.; Bos, P.; Hidding, J.; Feldbrugge, J.; ten Have, E.; van Engelen, M.; Caroli, M.; & Teillaud, M. 2011 Trans. Comput. Sci. XIV, pg. 60-101, special issue on Voronoi Diagrams and Delaunay Triangulation, eds. M. Gavrilova, C. Tan and M. Mostafavi (Springer)
- Varela, J., Betancort-Rijo, J., Trujillo, I., & Ricciardelli, E. 2012, ApJ, 744, 82
- Way, M.J., Gazis, P.R. & Scargle, J.S. 2011, ApJ, 727, 48
- White, S. D. M. 1979, MNRAS, 186, 145
- York, D.G., et al. 2000, AJ, 120, 1579
- Yu, J. & Peebles, J. 1969, ApJ, 158,103
- Zaninetti, L. 2012, Revista Mexicana de Astronomia y Astrofisica, 48, 209
- Zeldovich, Y.B. 1978, “The Theory of the Large Scale Structure of the Universe” in The large scale structure of the universe; Eds. M. Longair and J. Einasto, Proceedings of the Symposium, Tallin, Estonian SSR, September 12-16, 1977. (A79-13511 03-90) Dordrecht, D. Reidel Publishing Co., 1978, p.409

Zomorodian, A., 2005, *Topology for Computing*, volume 16 of *Cambridge Monographs on Applied and Computational Mathematics*. Cambridge University Press, New York, NY, 2005.

Zwidky, F, 1948, *The Observatory*, 68, 121

Zwidky, F, 1957, *Morphological Astronomy*, Springer-Verlag: Berlin